SUPPLEMENTARY INFORMATION

Table of contents

1. Experimental Details

1.1 General Information

All manipulations of air-sensitive materials were performed with the rigorous exclusion of oxygen and moisture in Schlenk-type glassware, either on a dual-manifold Schlenk line interfaced to a high-vacuum (10^{-3} mbar) line or in an argon-filled MBraun glovebox. Acetonitrile (MeCN) was destilled from CaH_2 under a nitrogen atmosphere and stored over molecular sieves (3 Å). THF was distilled under a nitrogen atmosphere from potassium and benzophenone prior to use. Hydrocarbon solvents (*n*-pentane, Et_2O) were dried using a MBraun solvent purification system (SPS-800). Deuterated solvents were obtained from Aldrich GmbH (99 atom% D) and were degassed and dried. NMR spectra were recorded on Bruker Avance II 300 or 400 MHz NMR and Ascend 400 MHz FT-NMR spectrometers. Chemical shifts are referenced to internal solvent resonances and are reported relative to tetramethylsilane (^{1}H, $^{13}C\{^{1}H\}$), 85 % H_3PO_4 ($^{31}P\{^{1}H\}$) and $CFCl_3$ (^{19}F). IR spectra were obtained on a Bruker Tensor 37 instrument. EI mass spectra were recorded at 70 eV on a Thermo Fisher Scientific DFS – Magnetic Sector GC/MS instrument. ESI mass spectra were obtained using a FT-ICR (Fourier transform ion cyclotron resonance) IonSpec Ultima mass spectrometer equipped with a 7T magnet (Cryomagnetics) or on a LTQ Orbitrap XL Q Exactive mass spectrometer (Thermo Fisher Scientific, San Jose, CA, USA) equipped with an HESI II probe. The instrument was calibrated in the m/z range 74-1822 using premixed calibration solutions (Thermo Scientific). A constant spray voltage of 4.6 kV, a dimensionless sheath gas of 8, and a dimensionless auxiliary gas flow rate of 2 were applied. The capillary temperature and the S-lens RF level were set to 320 °C and 62.0, respectively. Elemental analyses were performed on an Elementar microcube instrument.

PL measurements were performed with a Horiba JobinYvon Fluorolog-322 spectrometer equipped with a closed-cycle optical cryostat (Leybold) operating within a temperature range of 15-300K. Several measurements at temperatures down to 3.7 K were done with a pulse tube cryostat (Cryomech) apparatus. A Hamamatsu R9910 photomultiplier was used as detector for the emission spectral range of about 300-830 nm. The solid samples (crystalline solids) were measured as dispersions in a thin layer of viscous polyfluoroester oil (ABCR) placed between two 1 mm quartz plates. The latter were mounted on the cold finger of the cryostat. All emission spectra were corrected for the wavelength-dependent response of the spectrometer and detector (in relative photon flux units). Emission decay traces were recorded by connecting a photomultiplier to a 500 MHz LeCroy LT322 oscilloscope (typically via a 500 Ohm load for μsec-fast decays) and using a nitrogen laser (~2 nsec, ~1 μJ per pulse) for pulsed excitation at 337 nm. Several hundred traces were usually acquired and averaged. PL efficiencies at ambient temperature were determined using an integrating sphere out of optical PTFE, which was installed into the sample chamber of the spectrometer, according to the method of de Mello et al.[1] The uncertainty of this measurement was estimated to be ±10%.

1.2 Synthesis

Synthesis of $P(O)Ph_2C{\equiv}CH$ (**1**):

To a solution of ethynyldiphenylphosphine (1.00 g, 4.76 mmol, 1.00 eq.) in Et_2O (40 mL), aqueous H_2O_2 (30 %) (0.50 mL, 4.76 mmol, 1.00 eq.) in water (20 mL) was added dropwise. The mixture was stirred vigorously for 3 h. The organic phase was separated and the aqueous phase was extracted with Et_2O (2x 10 mL). The combined organic layers were washed with a 0.1 M solution of $Na_2S_2O_3$ and water and dried over Na_2SO_4. The solvent was removed under reduced pressure to yield **1** as a brown oil. Yield: 1.02 g (95 %).

Characterization data are consistent with literature values.[2] Additional data:

^{1}H NMR (300 MHz, $CDCl_3$, 298 K): δ [ppm] = 7.90-7.76 (m, 4H, Ph^{meta}), 7.58-7.41 (m, 6H, $Ph^{ortho,para}$), 3.36 (d, $^3J_{HP}$ = 9.7 Hz, 1H, C≡C-*H*). – **^{13}C{^{1}H} NMR** (75 MHz, $CDCl_3$, 298 K): δ [ppm] = 132.5 (d, $^4J_{CP}$ = 3.0 Hz, Ph^{para}), 132.2 (d, $^1J_{CP}$ = 122.1 Hz, Ph^{ipso}), 130.9 (d, $^2J_{CP}$ = 11.3 Hz, Ph^{ortho}), 128.7 (d, $^3J_{CP}$ = 13.6 Hz, Ph^{meta}), 94.2 (d, $^1J_{CP}$ = 28.8 Hz, P-*C*≡C), 79.9 (P-C≡*C*). – **^{31}P{^{1}H} NMR** (121 MHz, $CDCl_3$, 298 K): δ [ppm] = 8.29 (s).

Synthesis of (1-benzyl-1H-1,2,3-triazol-4-yl)diphenylphosphine oxide (**2**):

A 100 mL flask was charged with sodium ascorbate (87.6 mg, 0.44 mmol, 0.10 eq.), $CuSO_4{\cdot}5H_2O$ (11.9 mg, 0.04 mmol, 0.01 eq.), benzylazide (636 mg, 4.77 mmol, 1.08 eq.) and **1** (1.00 g, 4.42 mmol, 1.00 eq.). *t*BuOH/H_2O (20 mL; v/v = 1:1) was added and the mixture was stirred at room temperature for 3 days. The formed precipitate was isolated by filtration, dissolved in CH_2Cl_2 and dried over Na_2SO_4. The solvent was removed under reduced pressure to yield 2 as a colorless crystalline solid. Yield: 1.24 g (78 %).

Characterization data are consistent with literature values.[2] NMR spectra are shown in Figures S16-19.

Synthesis of 1-benzyl-4-(diphenylphosphoryl)-3-methyl-1H-1,2,3-triazol-3-ium trifluoromethanesulfonate (**3**):

Compound **2** (1.43 g, 3.98 mmol, 1.00 eq.) was dissolved in CH_2Cl_2 (50 mL) and cooled to -78° C. MeOTf (686 mg, 0.46 mL, 4.18 mmol, 1.05 eq.) was added dropwise. The solution was stirred over night when the solvent was concentrated to a volume of 5 mL under reduced pressure. The colorless product was precipitated by addition of Et_2O (15 mL), filtered and dried under reduced pressure. Yield: 2.09 g (98 %). Some impurities were detected in the NMR spectra. However, compound **3** was used without further purification.

^{1}H NMR (300 MHz, $CDCl_3$, 298 K): δ [ppm] = 8.34 (s, 1H, triazole-C*H*), 8.00-7.30 (m, 15H, H^{arom}), 5.87 (s, 2H, CH_2), 4.28 (s, 3H, NCH_3). – **^{13}C{^{1}H} NMR** (75 MHz, $CDCl_3$,

298 K): δ [ppm] = 138.0 (d, $^{1}J_{CP}$ = 92.9 Hz, P-triazole-*C*-CH), 134.4 (P-Ph-C^{para}), 133.2 (d, $^{1}J_{CP}$ = 20.2 Hz, P-Ph-*C*^{ispo}), 131.7 (d, $^{3}J_{CP}$ = 11.0 Hz, P-Ph-*C*^{meta}), 130.8 (CH_2Ph-*C*^{ipso}), 130.5 (d, $^{2}J_{CP}$ = 14.3 Hz, P-triazole-C-*C*H), 130.2 (CH_2Ph-*C*$^{ortho/meta}$), 130.0 (CH_2Ph-*C*^{para}), 129.8 (CH_2Ph-*C*$^{ortho/meta}$), 129.6 (d, $^{2}J_{CP}$ = 13.5 Hz, P-Ph-*C*^{ortho}), 58.2 (*C*H_2), 40.6 (N*C*H_3). – **^{31}P{^{1}H} NMR** (121 MHz, $CDCl_3$, 298 K): δ [ppm] = 16.0 (s). – **^{19}F NMR** (282 MHz, $CDCl_3$, 298 K): δ [ppm] = -78.3 (s). – **ESI-MS** (positive): *m/z* = [M]+ calcd. 374.1422; found: 374.1390. – **IR (ATR)**: $\tilde{\nu}$ [cm^{-1}] = 3116 (s), 3058 (s), 2362 (s), 2335 (s), 1589 (w), 1532 (w), 1496 (w), 1439 (s), 1379 (w), 1275 (vs), 1250 (vs), 1214 (vs), 1152 (vs), 1121 (vs), 1078 (vw), 1027 (vs), 996 (w), 932 (vw), 826 (vw), 731 (vs), 695 (vs), 633 (vs), 557 (vs), 525 (vs), 484 (w), 463 (w), 439 (vw). – **Elemental Analysis**: calcd. (%) for $C_{23}H_{21}N_3F_3O_3PS$: N 8.03, C 52.77, H 4.04, S 6.13; found: N 7.77, C 51.34, H 3.93, S 6.76.

Synthesis of L^{PN} (**4**):

A suspension of **2** (4.00 g, 11.1 mmol, 1.00 eq.) in toluene (6 mL) was added $PhSiH_3$ (5.50 mL, 44.5 mmol, 4.00 eq.) and heated to 110° C for 8 days. Volatiles were removed under reduced pressure and the resulting solid was recrystallized from hot EtOH to yield the product as a colorless crystalline solid. Yield: 2.21 g (58 %).

Characterization data are consistent with literature values.[3] NMR spectra are shown in Figures S21-23.

Synthesis of L^{PC}H^{+} OTf^{-} (**5**):

A suspension of **3** (1.08 g, 2.06 mmol, 1.00 eq.) in toluene (3.50 mL) was added $PhSiH_3$ (2.10 mL, 16.5 mmol, 8.00 eq.) and heated to 110° C for 6 days. Volatiles were removed under reduced pressure and the resulting solid was recrystallized from hot toluene to yield the product as a colorless crystalline solid. Yield: 711 mg (68 %).

^{1}H NMR (300 MHz, $CDCl_3$, 298 K): δ [ppm] = 7.88 (s, 1H, triazole-C*H*), 7.34-7.57 (m, 15H, H^{arom}), 5.82 (s, 2H, CH_2), 4.06 (s, 3H, NCH_3). – **^{13}C{^{1}H} NMR** (75 MHz, $CDCl_3$, 298 K): δ [ppm] = 144.8 (d, $^{1}J_{CP}$ = 36.0 Hz, P-triazole-*C*-CH), 134.4 (d, $^{2}J_{CP}$ = 22.1 Hz, P-triazole-C-*C*H), 134.3 (P-Ph-C^{para}), 132.8 (d, $^{1}J_{CP}$ = 11.3 Hz, P-Ph-*C*^{ipso}), 131.4 (CH_2Ph-*C*^{ipso}, overlapping with P-Ph-*C*^{meta}), 131.3 (d, $^{3}J_{CP}$ = 13.9 Hz, P-Ph-*C*^{meta}), 130.0 (CH_2Ph-*C*$^{ortho/meta}$), 129.9 (CH_2Ph-*C*^{para}), 129.8 (CH_2Ph-*C*$^{ortho/meta}$), 129.5 (d, $^{2}J_{CP}$ = 15.9 Hz, P-Ph-*C*^{ortho}), 57.8 (*C*H_2), 39.1 (d, $^{3}J_{CP}$ = 7.7 Hz, N*C*H_3). – **^{31}P{^{1}H} NMR** (121 MHz, $CDCl_3$, 298 K): δ [ppm] = -31.5 (s). – **^{19}F NMR** (282 MHz, $CDCl_3$, 298 K): δ (ppm) = -78.2 (s). – **ESI-MS** (positive): *m/z* = [M]+ calcd. 358.1473; found: 358.1516. – **IR (ATR)**: $\tilde{\nu}$ [cm^{-1}] = 3126 (w), 3054 (w), 3029 (w), 2361 (w), 2336 (w), 2172 (w), 1454 (w), 1434 (s), 1376 (w), 1275 (vs), 1252 (vs), 1225 (s), 1149 (vs), 1090 (w), 1028 (vs), 998 (w), 829 (w), 799 (vw), 735 (s), 694 (s), 632 (vs), 572 (w), 504 (s), 452 (w); 430 (vw). – **Elemental Analysis**: calcd. (%) for $C_{23}H_{21}N_3F_3O_3PS$: N 8.28, C 54.44, H 4.17, S 6.32; found: N 7.93, C 53.94, H 3.97, S 6.69.

Synthesis of [AuCl(L^{PN})] (**6**):

A 50 mL flask was charged with [AuCl(tht)] (934 mg, 2.91 mmol, 1.00 eq.) and **4** (1.00 g, 2.91 mmol, 1.00 eq.) and CH_2Cl_2 (10 mL) was added. The mixture was stirred for 1 h at room temperature. The solvent was removed under reduced pressure and the product was washed with Et_2O (10 mL) and dried. Yield: 1.22 g (73 %).

^{1}H NMR (300 MHz, $CDCl_3$, 298 K): *δ* [ppm] = 8.13 (s, 1H, triazole-C*H*), 7.82-7.73 (m, 4H, H^{arom}), 7.53-7.29 (m, 11H, H^{arom}), 5.58 (s, 2H, CH_2). – **^{13}C{^{1}H} NMR** (75 MHz, $CDCl_3$, 298 K): *δ* [ppm] = 137.4 (d, $^1J_{CP}$ = 89.5 Hz, P-Ph^{ipso}), 134.0 (d, $^2J_{CP}$ = 14.4 Hz, P-Ph^{ortho}), 133.4 (CH_2-Ph^{ipso}), 132.5 (d, J_{CP} = 38.5, P-Ph), 132.1 (d, J_{CP} = 2.7 Hz, P-Ph), 129.5, 129.4, 129.2 (d, J_{CP} = 12.6 Hz, P-Ph), 128.5 (d, J_{CP} = 68.3 Hz, P-Ph), 128.4, 54.6 (*C*H_2). – **^{31}P{^{1}H} NMR** (121 MHz, $CDCl_3$, 298 K): *δ* [ppm] = 6.96 (s). – **EI-MS**: *m/z* = [M]+ calcd. 575.0592; found: 575.0246. – **IR (ATR)**: *ṽ* [cm^{-1}] = 3118 (w), 3060 (vw), 1586 (vw), 1493 (w), 1455 (vw), 1434 (s), 1365 (vw), 1308 (vw), 1209 (w), 1184 (vw), 1141 (vw), 1103 (vs), 1046 (w), 1027 (vw), 997 (w), 864 (w), 764 (s), 690 (vs), 659 (w), 554 (vs), 520 (s), 484 (s). – **Elemental Analysis**: calcd. (%) for $C_{21}H_{18}AuClN_3P$: N 7.30, C 43.81, H 3.15; found: N 6.96, C 43.47, H 3.39.

Synthesis of [AuCl(L^{PC}H)]OTf (**7**):

A 50 mL flask was charged with **5** (50.0 mg, 0.10 mmol, 1.00 eq.) and [AuCl(tht)] (31.6 mg, 0.10 mmol, 1.00 eq.) and CH_2Cl_2 (5 mL) was added. The solution was stirred for 2 h at room temperature and the solvent was concentrated under reduced pressure. Addition of *n*-pentane (10 mL) leads to the precipitation of the crude product, which was isolated by filtration and dried. Yield: 50.3 mg (68 %).

^{1}H NMR (300 MHz, $CDCl_3$, 298 K): *δ* [ppm] = 7.95 (s, 1H, triazole-C*H*, overlapping with H^{arom}), 7.36-8.03 (m, 15H, H^{arom}), 5.88 (s, 2H, CH_2), 4.16 (s, 3H, NCH_3). – **^{13}C{^{1}H} NMR** (75 MHz, $CDCl_3$, 298 K): *δ* [ppm] = 136.4 (d, $^1J_{CP}$ = 10.6 Hz, triazole-*C*-CH), 135.0 (triazole-*C*H), 134.8 (P-Ph-C^{para}), 134.7 (CH_2-Ph-C^{ipso}), 130.8 (d, J_{CP} = 13.5 Hz, P-C^{arom}), 130.4 (CH_2-Ph-*C*), 130.2 (CH_2-Ph-*C*), 129.8 (d, J_{CP} = 15.5 Hz, P-C^{arom}), 122.6 (CH_2-Ph-*C*), 121.7 (CH_2-Ph-*C*), 58.8 (s, *C*H_2), 40.6 (s, N*C*H_3). – **^{31}P{^{1}H} NMR** (121 MHz, $CDCl_3$, 298 K): *δ* [ppm] = 12.1 (s). – ^{19}F NMR (282 MHz, $CDCl^3$, 298 K): *δ* [ppm] = -78.2 (s). – **ESI-MS** (positive): *m/z* = [M]+ calcd. 590.0827; found: 590.0980. – **IR (ATR)**: *ṽ* [cm^{-1}] = 3112 (vw), 3036 (vw), 2362 (vs), 2335 (vs), 1769 (vw), 1736 (vw), 1694 (vw), 1678 (vw), 1652 (vw), 1577 (vw), 1559 (vw), 1437 (s), 1258 (vs), 1226 (s), 1197 (w), 1150 (vs), 1098 (s), 1028 (vs), 998 (vw), 784 (vw), 735 (w), 693 (w), 632 (s), 573 (w), 514 (s), 462 (w). – **Elemental Analysis**: calcd. (%) for $C_{23}H_{21}AuClN_3F_3O_3PS$: N 5.68, C 37.34, H 2.86, S 4.33; found: N 5.63, C 37.65, H 2.83, S 4.78.

Synthesis of [Cu(AuCl(L^{PN}))$_2$(thf)$_2$]PF_6 (**8**):

A 50 mL flask was charged with **6** (100 mg, 0.27 mmol, 1.00 eq.) and [Cu(MeCN)$_4$]PF_6 (32.2 mg, 0.13 mmol, 0.50 eq.) and CH_2Cl_2 (10 mL) was added. The solution was stirred over night at room temperature when the solvent was removed under reduced

pressure. The pure product was obtained by slow evaporation of a THF solution. Yield: 31.4 mg (26 %).

^{1}H NMR (300 MHz, $CDCl_3$, 298 K): δ [ppm] = 7.95 (s, 2H, triazole-C*H*), 7.66-7.29 (m, 30H, H^{arom}), 5.63 (s, 4H, CH_2). – **^{13}C{^{1}H} NMR** (75 MHz, $CDCl_3$, 298 K): δ [ppm] = 133.9 (d, J_{CP} = 14.6 Hz, P-C^{arom}), 133.0 (d, J_{CP} = 2.4 Hz, P-C^{arom}), 132.6, 132.0 (d, J_{CP} = 15.6 Hz, P-C^{arom}), 129.8 (d, J_{CP} = 12.9 Hz, P-C^{arom}), 129.4, 129.3, 129.0, 125.8 (CH_2-Ph-*C*), 125.0 (CH_2-Ph-*C*), 68.0 (thf), 55.9 (CH_2), 25.6 (thf). – **^{31}P{^{1}H} NMR** (121 MHz, $CDCl_3$, 298 K): δ [ppm] = 12.6 (s, *P*-AuCl), -144.2 (sept, $^{1}J_{PF}$ = 713.6 Hz, PF_6). – **^{19}F NMR** (282 MHz, $CDCl_3$, 298 K): δ [ppm] = -72.0 (d, $^{1}J_{FP}$ = 713.5 Hz, PF_6). – **ESI-MS** (positive): *m/z* = $[Cu(AuCl(L^{PN})_2]^+$ calcd. 1213.0481, $[(AuCl(L^{PN}))_2\text{-}Cl]^+$ calcd. 1115.1496; found: 1213.0468, 1115.1481. – **IR (ATR)**: $\tilde{\nu}$ [cm^{-1}] = 1497 (w), 1482 (vw), 1456 (vw), 1437 (s), 1124 (vw), 1102 (s), 1070 (vw), 1027 (vw), 998 (vw), 833 (vs), 745 (w), 715 (s), 700 (w), 689 (vs), 658 (w), 618 (vw), 584 (vw), 556 (vs), 549 (w), 521 (vs), 484 (s), 455 (vw). – **Elemental Analysis**: calcd. (%) for $C_{42}H_{36}Au_2Cl_2CuF_6N_6P_3$ (M – 2 THF): N 6.18, C 37.09, H 2.67; found: N 6.21, C 37.04, H 2.89.

Synthesis of $[Au_2(L^{PC})_2](OTf)_2$ (**9**):

A 50 mL flask was charged with **7** (356 mg, 0.48 mmol, 1.00 eq.) and AgOAc (80.3 mg, 0.48 mmol, 1.00 eq.) and CH_2Cl_2 (10 mL) was added. The mixture was stirred for 1 h and the precipitate (AgCl) was removed by filtration. The solvent was removed under reduced pressure and the resulting crude product was recrystallized from MeCN. Yield: 160 mg (47 %).

^{1}H NMR (300 MHz, CD_3CN, 298 K): δ [ppm] = 7.80-7.51 (m, 22H, H^{arom}), 7.42-7.36 (m, 4H, H^{arom}), 7.16-7.12 (m, 4H, H^{arom}), 5.71 (s, 4H, CH_2), 3.69 (s, 6H, NCH_3). – **^{13}C{^{1}H} NMR** (75 MHz, CD_3CN, 298 K): δ [ppm] = 133.6, 133.5 (d, J_{CP} = 14.7 Hz, P-C^{arom}), 133.4 (d, J_{CP} = 2.7 Hz, P-C^{arom}), 130.2 (d, J_{CP} = 12.3 Hz, P-C^{arom}), 129.4, 129.2 (d, J_{CP} = 29.7 Hz, P-C^{arom}), 123.0, 122.3, 58.4 (CH_2), 40.4 (NCH_3). Due to low solubility, some carbon resonances could not be detected. – **^{31}P{^{1}H} NMR** (121 MHz, CD_3CN, 298 K): δ [ppm] = 21.1 (s). – **^{19}F NMR** (282 MHz, CD_3CN, 298 K): δ [ppm] = 79.3 (s). – **ESI-MS** (positive): *m/z* = $[(Au(L^{PC})_2]^{2+}$ calcd. 554.1060; found: 554.1051. – **IR (ATR)**: $\tilde{\nu}$ [cm^{-1}] = 3047 (vw), 1482 (vw), 1460 (vw), 1438 (w), 1433 (vw), 1415 (vw), 1313 (vw), 1273 (vw), 1262 (vs), 1224 (s), 1187 (vw), 1152 (vs), 1097 (w), 1033 (vs), 996 (vw), 921 (vw), 852 (vw), 829 (vw), 798 (w), 755 (vw), 749 (w), 740 (s), 720 (vw), 708 (s), 694 (w), 679 (vw), 662 (vw), 637 (vs), 592 (w), 572 (w), 553 (s), 516 (vs), 491 (w), 477 (s), 458 (w), 450 (vw), 427 (vw). – **Elemental Analysis**: calcd. (%) for $C_{46}H_{40}Au_2F_6N_6P_2S_2$: N 5.97, C 39.27, H 2.87, S 4.56; found: N 6.29, C 39.82, H 3.10, S 4.39.

2. Crystallographic Appendix

2.1 Single Crystal X-ray Diffraction

A suitable crystal was covered in mineral oil (Aldrich) and mounted on a glass fiber. The crystal was transferred directly to the cold stream of a STOE IPDS 2 or a STOE StadiVari diffractometer. All structures were solved by using the programs SHELXS/T[4,5] and Olex2.[6] The remaining non-hydrogen atoms were located from successive difference Fourier map calculations. The refinements were carried out by using full-matrix least-squares techniques on F^2 by using the program SHELXL.[4,5] In each case, the locations of the largest peaks in the final difference Fourier map calculations, as well as the magnitude of the residual electron densities, were of no chemical significance.

Crystallographic data (excluding structure factors) for the structures reported in this paper have been deposited with the Cambridge Crystallographic Data Centre as a supplementary publication no. 1901789-1901794. Copies of the data can be obtained free of charge on application to CCDC, 12 Union Road, Cambridge CB21EZ, UK (fax: (+(44)1223-336-033; email: deposit@ccdc.cam.ac.uk).

In the crystal structure of compound **6**, disordered tetrahydrothiophene and CH_2Cl_2 molecules were observed and refined as shown in Fig. S1.

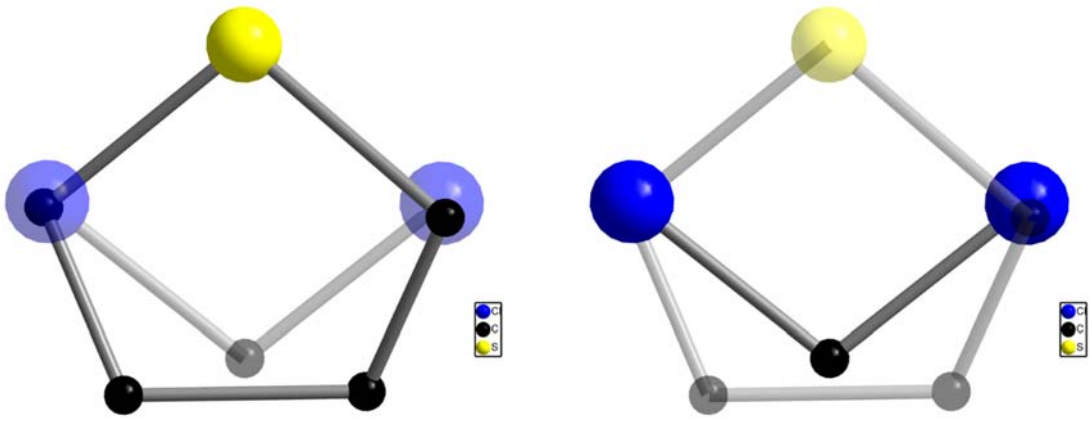

Figure S1. Disorder of tetrahydrothiophene and CH_2Cl_2 in the crystal structure of **6**.

2.1 Crystal Data

Table S1. Crystal data of compounds **2**, **6**, **7** and **8**.

Compound	**2**	**6**· 0.35 THT · 0.65 CH_2Cl_2	**7** · 0.75 CH_2Cl_2	**8** · 2 THF
Formula	$C_{21}H_{18}N_3OP$	$C_{21}H_{18}AuClN_3P$ · 0.35 THT · 0.65 CH_2Cl_2	$C_{23}H_{21}AuClF_3N_3O_3PS$ · 0.75 CH_2Cl_2	$C_{50}H_{52}Au_2Cl_2CuF_6N_6O_2P_3$ · 2 THF
$D_{calc.}$/ g cm^{-3}	1.274	1.821	1.876	1.769
μ/mm^{-1}	0.161	6.462	5.587	5.33
Formula Weight / g mol^{-1}	359.35	661.83	803.57	1648.46
Colour	colourless	colourless	colourless	colourless
Shape	needle	block	needle	block
Size/mm^3	0.58×0.46×0.26	0.35×0.25×0.15	0.48×0.35×0.19	0.41×0.33×0.25
T/K	200	100	150	100
Crystal System	monoclinic	trigonal	monoclinic	monoclinic
Flack Parameter		-0.009(10)		
Hooft Parameter		0.005(6)		
Space Group	$P2_1/n$	$P3_121$	$P2_1/n$	$P2_1/n$
a/Å	13.9345(6)	10.9905(2)	22.5105(5)	10.3665(4)
b/Å	9.7852(3)		11.1318(2)	27.9101(11)
c/Å	14.3148(6)	34.6093(8)	23.4398(6)	21.4135(7)
α/°				
β/°	106.293(3)		104.362(2)	92.509(3)
γ/°				
V/Å^3	1873.46(13)	3620.41(16)	5690.0(2)	6189.6(4)
Z	4	6	8	4
Z'	1	1	2	1
Wavelength/Å	0.71073	0.71073	0.71073	0.71073
Radiation type	MoK_α	MoK_α	MoK_α	MoK_α
Θ_{min}/°	1.802	1.765	1.794	1.459
Θ_{max}/°	29.575	28.970	29.527	30.066
Measured Refl.	14127	22207	33022	34254
Independent Refl.	5093	5723	15774	14732
Reflections with I > 2(I)	4182	5205	13642	9808
R_{int}	0.0250	0.0425	0.0265	0.0839
Parameters	235	309	690	797
Restraints	0	25	100	122
Largest Peak	0.402	1.822	1.634	2.906
Deepest Hole	-0.270	-0.948	-1.194	-1.569
GooF	1.037	1.091	1.082	1.134
wR_2 (all data)	0.1157	0.1056	0.0855	0.2401
wR_2	0.1089	0.1017	0.0799	0.2095
R_1 (all data)	0.0502	0.0453	0.0434	0.1263
R_1	0.0399	0.0399	0.0339	0.0831

Table S2. Crystal data for compounds **9** and **10**.

Compound	**9**	**10**
Formula	$C_{46}H_{40}Au_2F_6N_6O_6P_2S_2$	$C_{42}H_{34}Au_2N_6P_2$
$D_{calc.}$/ g cm^{-3}	1.972	1.970
μ/mm^{-1}	6.420	8.186
Formula Weight / g mol^{-1}	1406.83	1078.62
Colour	colourless	colourless
Shape	block	plate
Size/mm^3	0.38×0.25×0.13	0.18×0.14×0.09
T/K	100	150
Crystal System	triclinic	monoclinic
Space Group	P-1	$P2_1/c$
a/Å	9.4576(5)	8.4784(5)
b/Å	10.1973(5)	24.9135(9)
c/Å	13.0812(9)	8.7132(5)
α/°	97.575(5)	90
β/°	108.220(5)	98.792(4)
γ/°	91.529(4)	90
V/Å^3	1184.77(12)	1818.83(16)
Z	1	2
Z'	0.5	0.5
Wavelength/Å	0.71073	0.71073
Radiation type	MoK_α	MoK_α
Θ_{min}/°	2.020	1.635
Θ_{max}/°	29.943	27.196
Measured Refl.	11957	10005
Independent Refl.	5738	4031
Reflections with I > 2(I)	5327	3318
R_{int}	0.0260	0.0232
Parameters	317	235
Restraints	0	0
Largest Peak	2.039	1.094
Deepest Hole	-0.682	-0.704
GooF	1.012	1.005
wR_2 (all data)	0.0623	0.0565
wR_2	0.0617	0.0537
R_1 (all data)	0.0273	0.0341
R_1	0.0253	0.0236

2.2 Solid State Structures

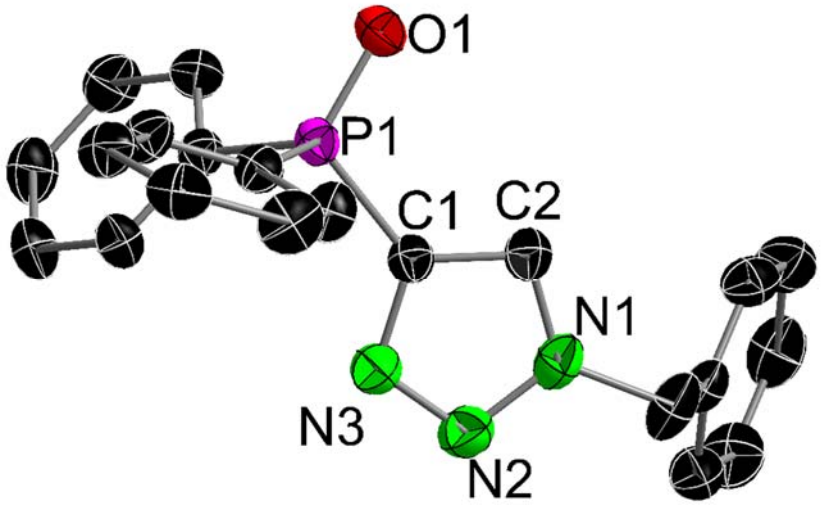

Figure S2. Molecular structure of **2** in the solid state. Thermal ellipsoids are drawn to encompass 50 % probability. Selected bond lengths [Å] and angles [°]: P1-O1 1.4909(9), P1-C1 1.7935(13), O1-P1-C1 110.02(6), N3-C1-P1 124.54(9).

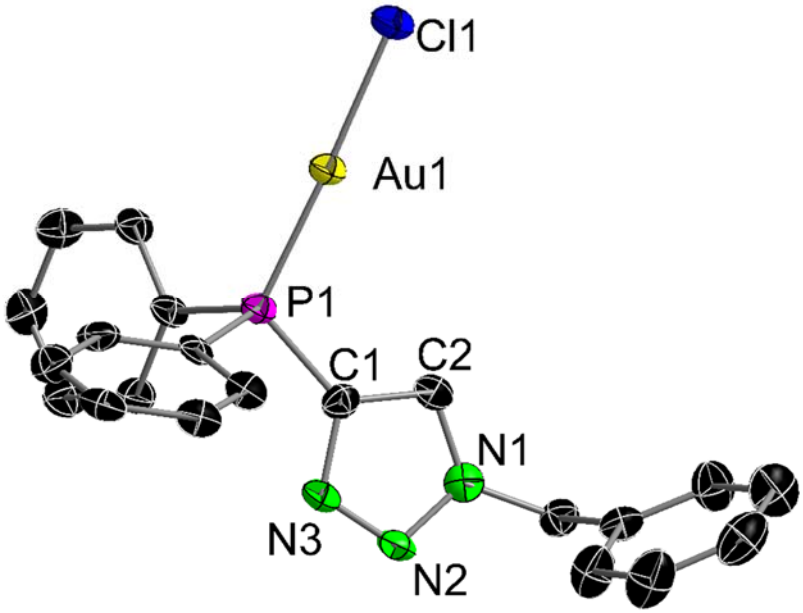

Figure S3. Molecular structure of **6** in the solid state. Thermal ellipsoids are drawn to encompass 50 % probability.

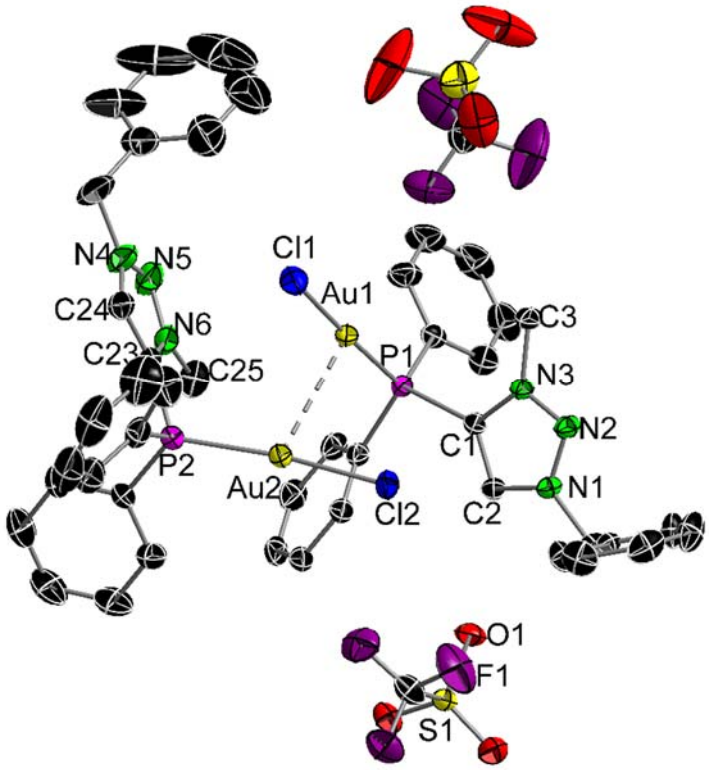

Figure S4. Molecular structure of **7** in the solid state. Thermal ellipsoids are drawn to encompass 50 % probability.

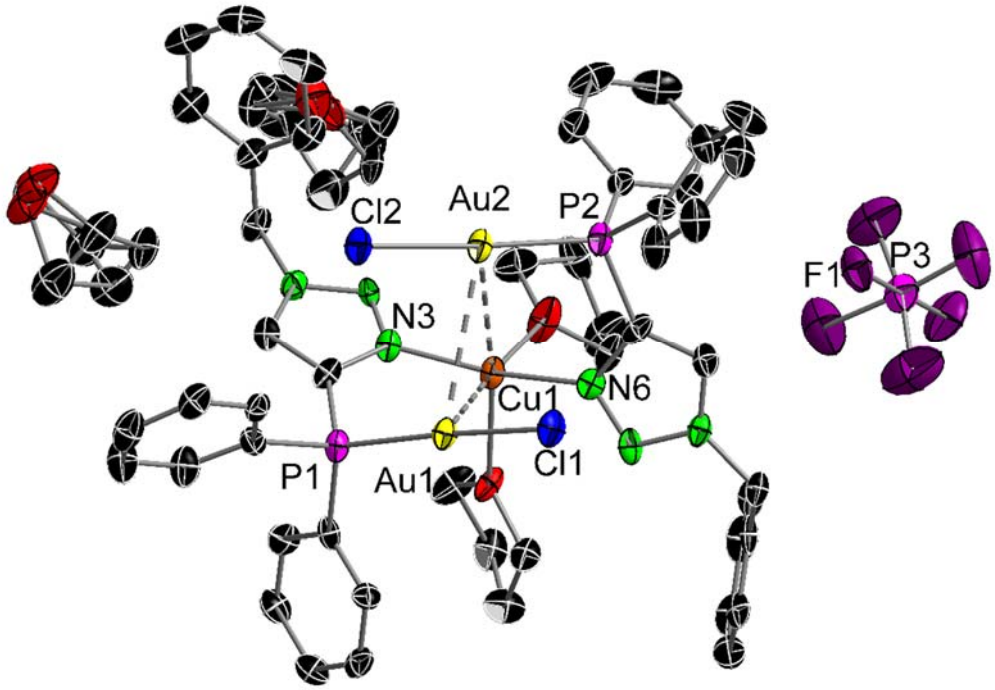

Figure S5. Molecular structure of **8** in the solid state. Thermal ellipsoids are drawn to encompass 50 % probability.

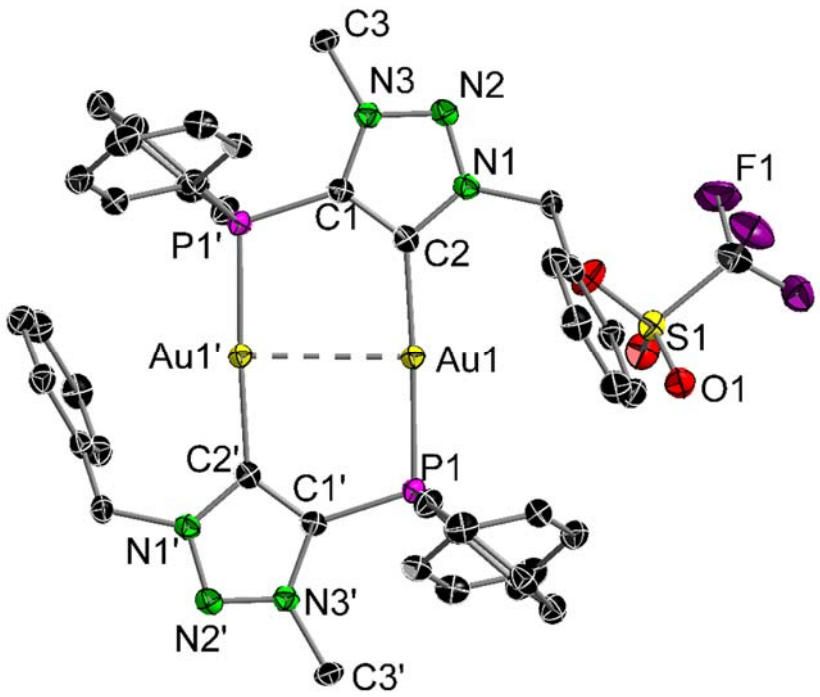

Figure S6. Molecular structure of **9** in the solid state. Thermal ellipsoids are drawn to encompass 50 % probability.

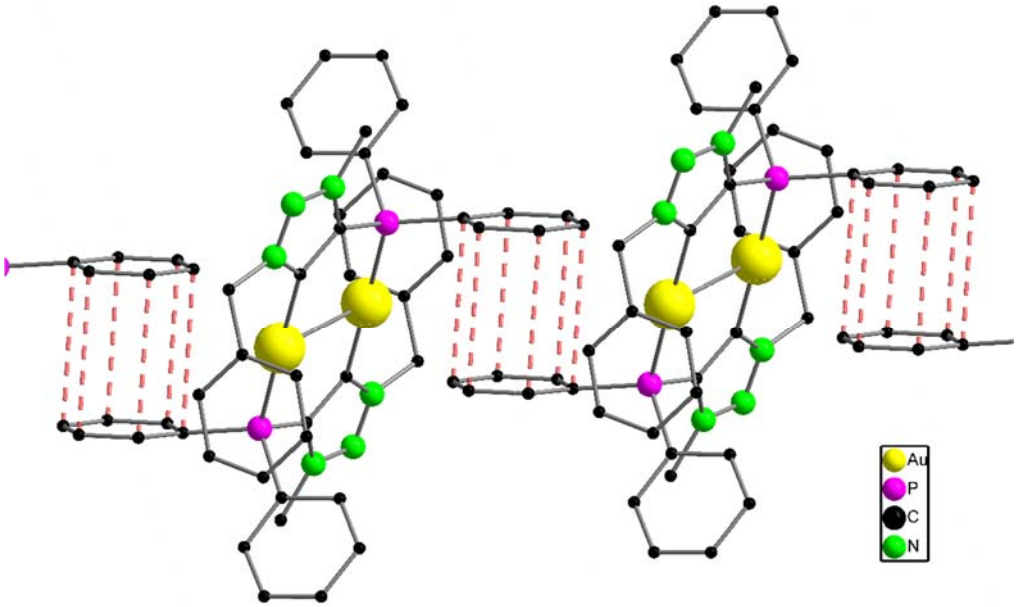

Figure S7. π-Stacking between the phenyl groups of **9** in the solid state. Shown are the only the cations. The distance between the phenyl groups is 3.8 Å.

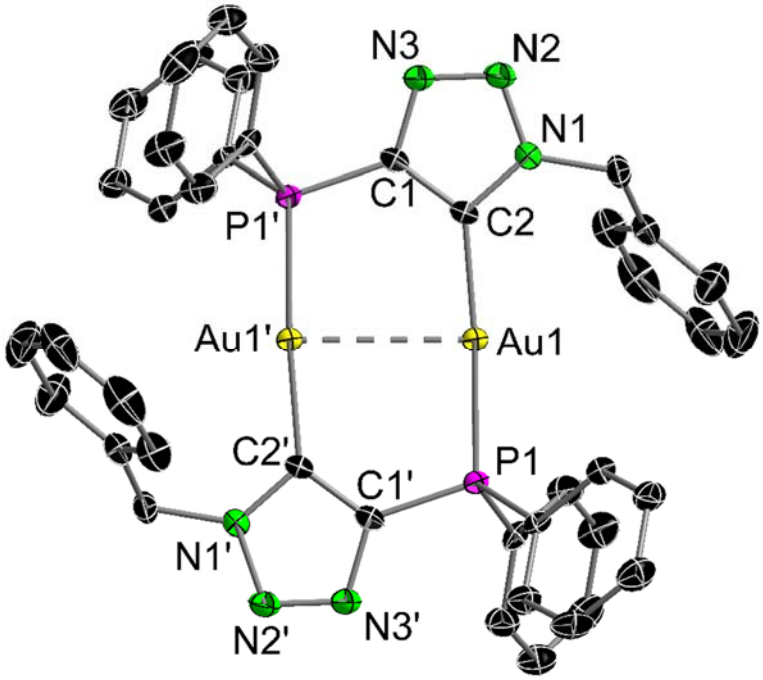

Figure S8. Molecular structure of **10** in the solid state. Thermal ellipsoids are drawn to encompass 50 % probability.

3. Photoluminescence data

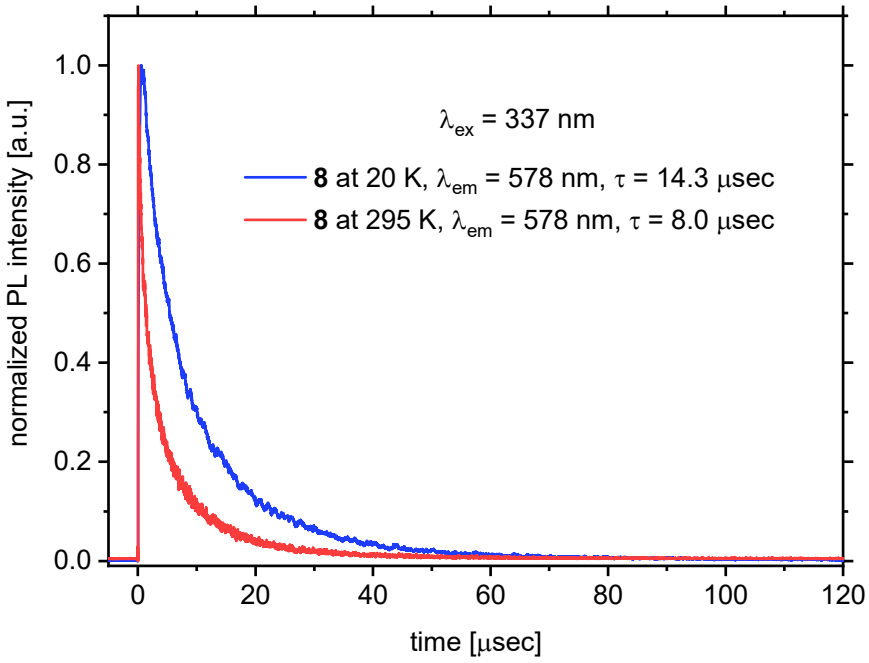

Figure S9. Decay curves of the broad emission (phosphorescence) of compound **8** at 20 and 295 K, recorded using an oscilloscope and nsec-pulsed excitation at 337 nm with a nitrogen laser (~2 nsec, ~1 μJ per pulse). The curves could be well fit with a monoexponential decay function with the indicated lifetimes.

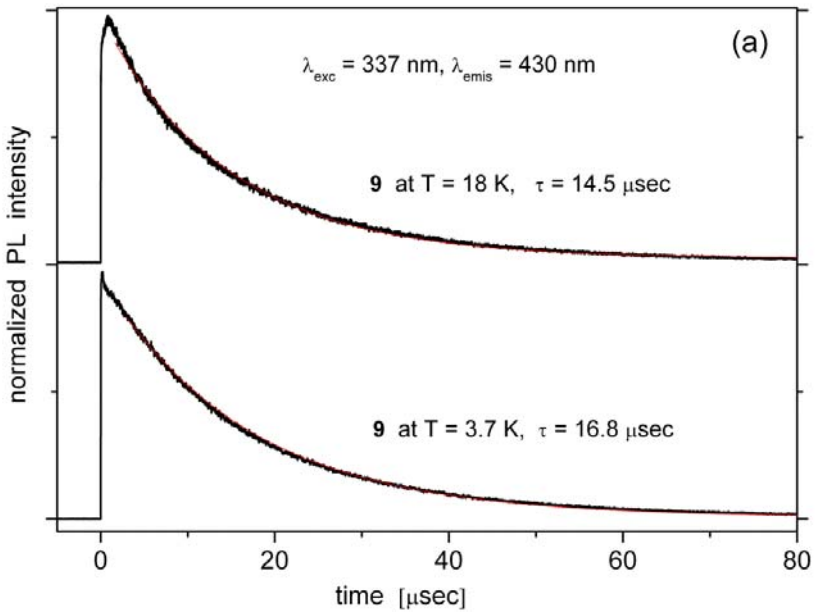

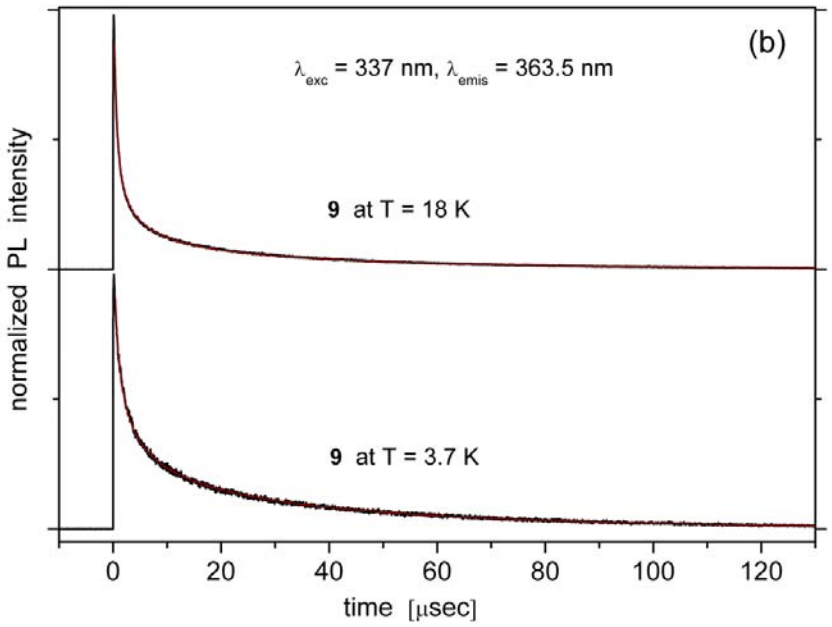

Figure S10. Emission decay curves of compound **9** at low temperatures for (a) the broad emission band at 430 nm and (b) the narrow exciton emission at 363 nm. These were recorded by using an oscilloscope and nsec-pulsed excitation at 337 nm with a nitrogen laser (~2 nsec, ~1 μJ per pulse). The red lines indicate fit curves following (a) monoexponential decay and (b) the stretched exponential function of the form $y = y_0 \times t^{-n} \times \exp(-t/\tau)$ (18 K: $n = 0.51$, $\tau =$ 70 μsec; 3.7 K: $n = 0.4$, $\tau = 62$ μsec).

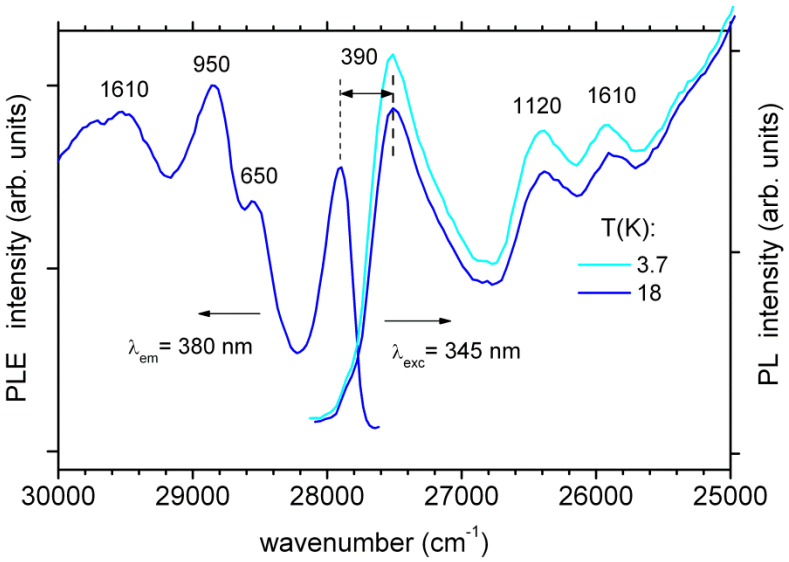

Figure S11. Low-temperature excitation (PLE) and emission (PL) spectra of solid (polycrystalline) compound **9** in the region of narrow PLE and PL bands at 358.4 and 363.5 nm (27902 and 27510 cm^{-1}), respectively. These bands show a Stokes shift of 390 cm^{-1} (*ca.* 50 meV). The higher-energy (PLE) and lower-energy (PL) subbands are ascribed to the phonon replica; their frequencies are indicated in cm^{-1}. The PLE and PL spectra were recorded using spectral slit widths of 1 nm (~80 cm^{-1} at $\nu = 28000$ cm^{-1}).

4. NMR Spectra

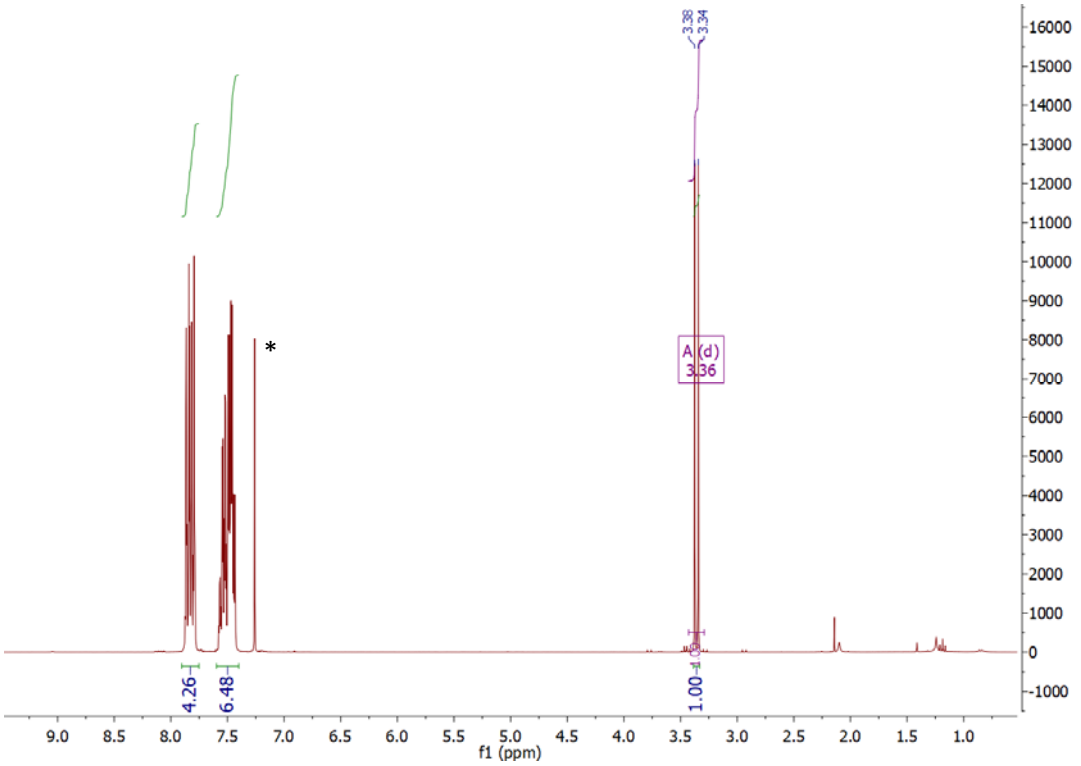

Figure S12. ^{1}H NMR (300 MHz, $CDCl_3$, 298 K) spectrum of **1** (* = solvent peak).

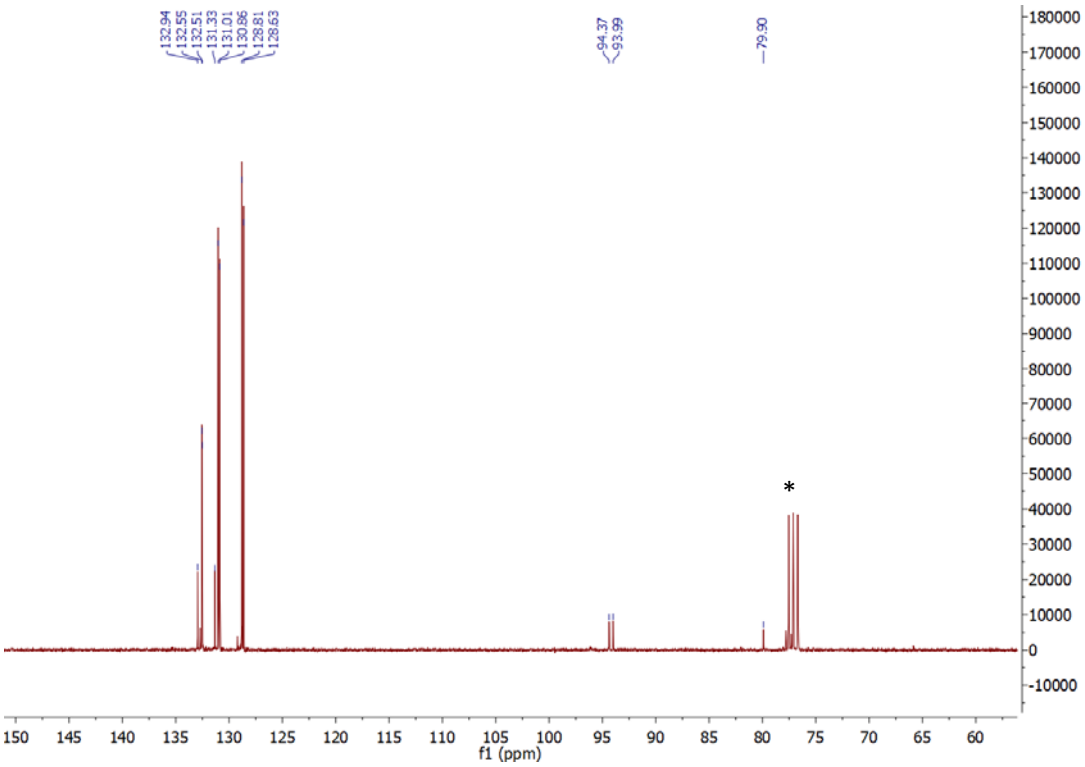

Figure S13. ^{13}C NMR (75 MHz, $CDCl_3$, 298 K) spectrum of **1** (* = solvent peak).

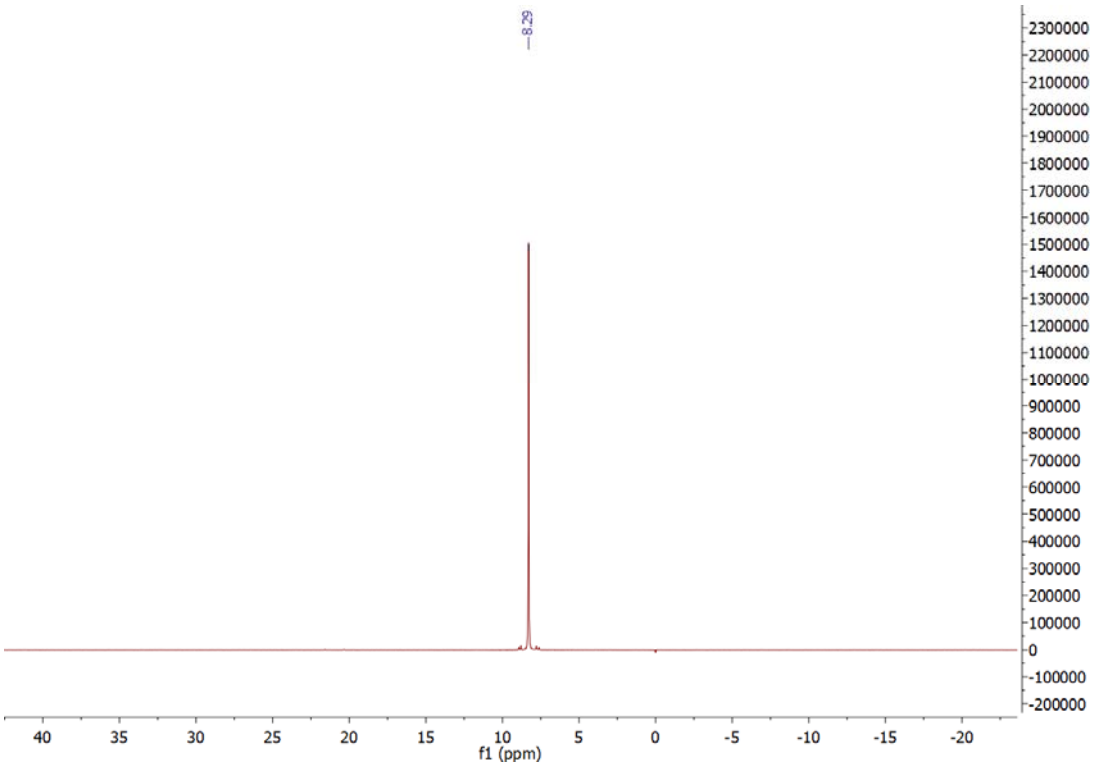

Figure S14. $^{31}P\{^{1}H\}$ NMR (121 MHz, $CDCl_3$, 298 K) spectrum of **1**.

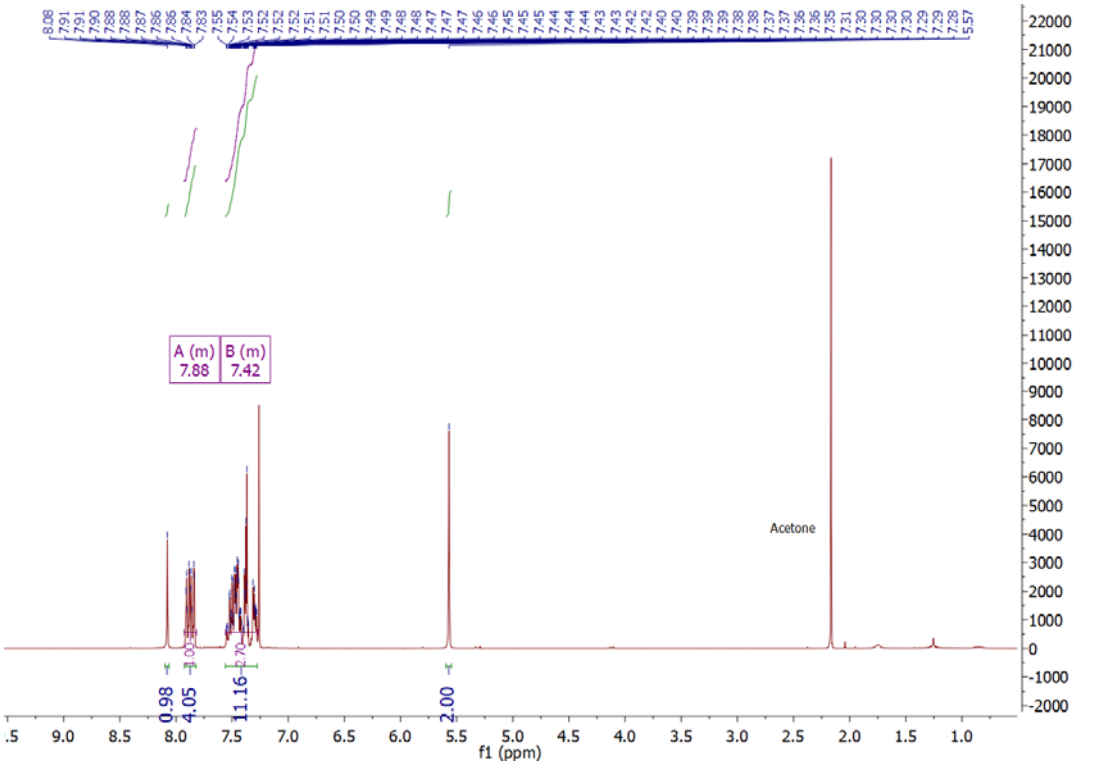

Figure S15. ^{1}H NMR (300 MHz, $CDCl_3$, 298 K) spectrum of **2**.

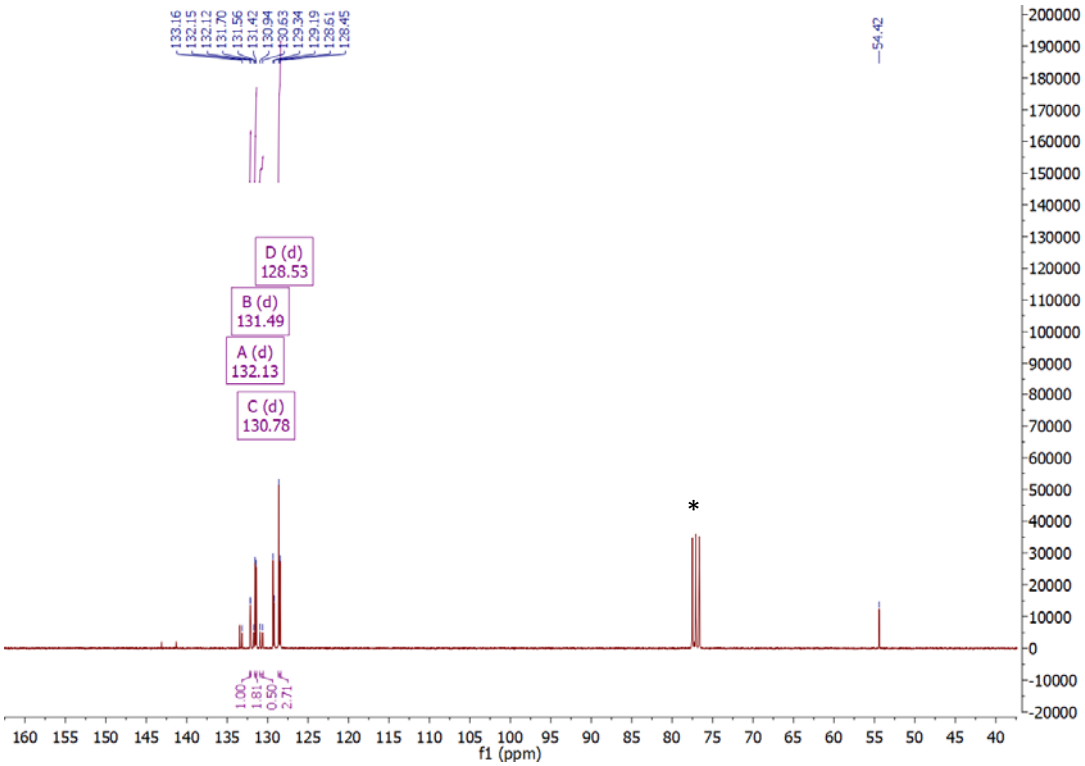

Figure S16. ^{13}C NMR (75 MHz, $CDCl_3$, 298 K) spectrum of **2** (* = solvent peak).

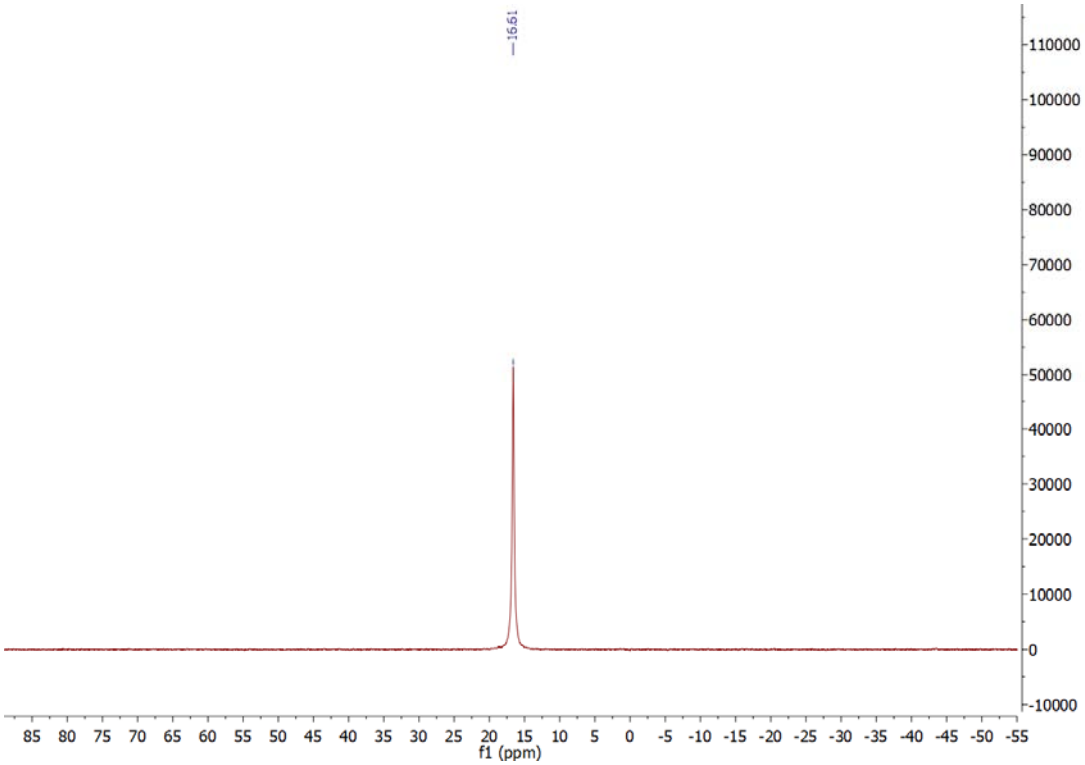

Figure S17. $^{31}P\{^1H\}$ NMR (121 MHz, $CDCl_3$, 298 K) spectrum of **2**.

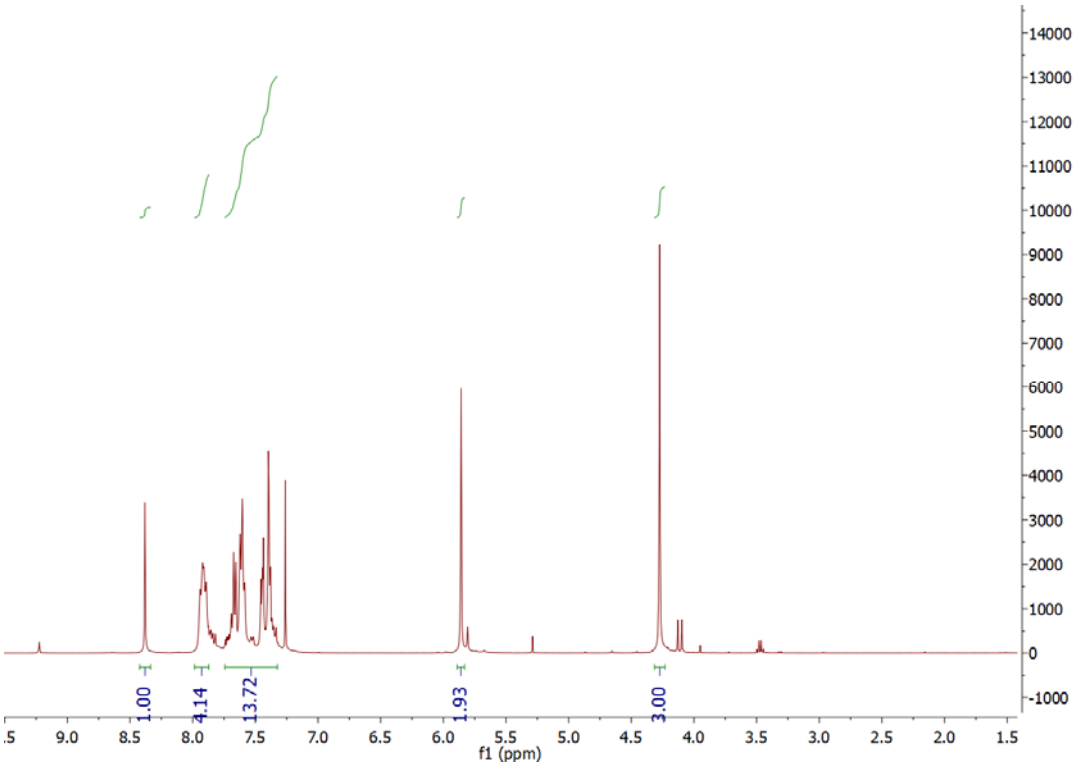

Figure S18. ^{1}H NMR (300 MHz, $CDCl_3$, 298 K) spectrum of **3**. The spectrum shows some impurities, which were not relevant for further reactions.

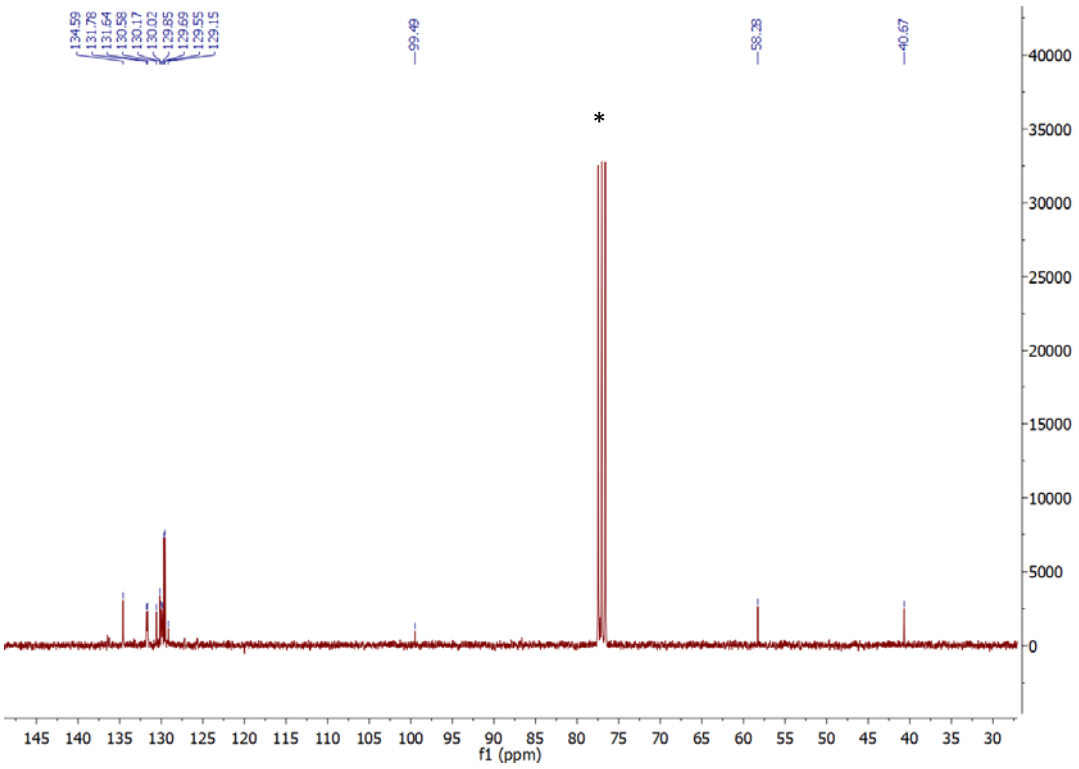

Figure S19. ^{13}C NMR (75 MHz, $CDCl_3$, 298 K) spectrum of **3** (* = solvent peak). The spectrum shows some impurities, which were not relevant for further reactions.

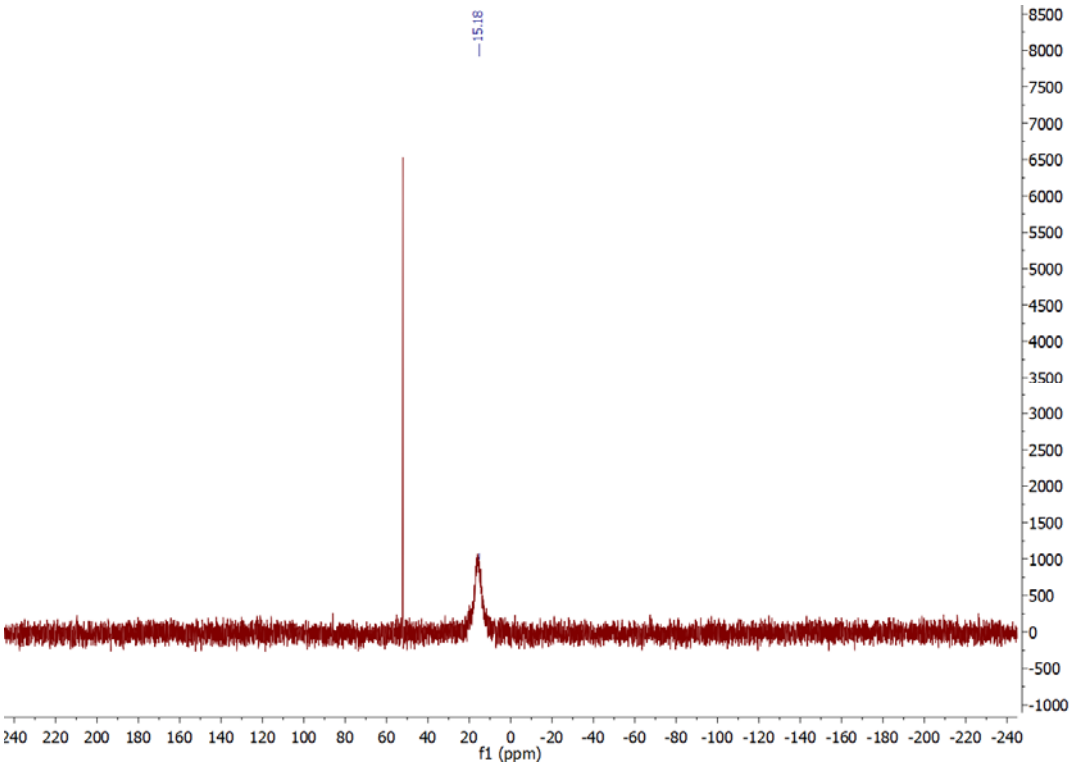

Figure S20. $^{31}P\{^{1}H\}$ NMR (121 MHz, $CDCl_3$, 298 K) spectrum of **3**. The spectrum shows some impurities, which were not relevant for further reactions.

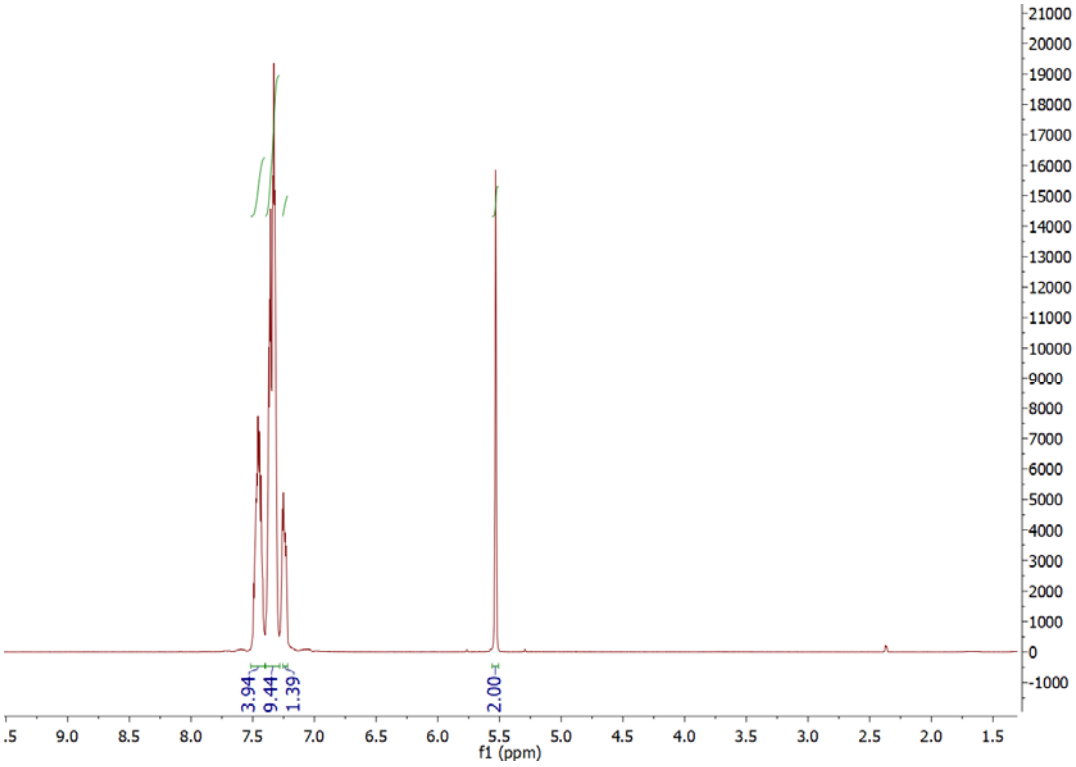

Figure S21. ^{1}H NMR (300 MHz, $CDCl_3$, 298 K) spectrum of **4**.

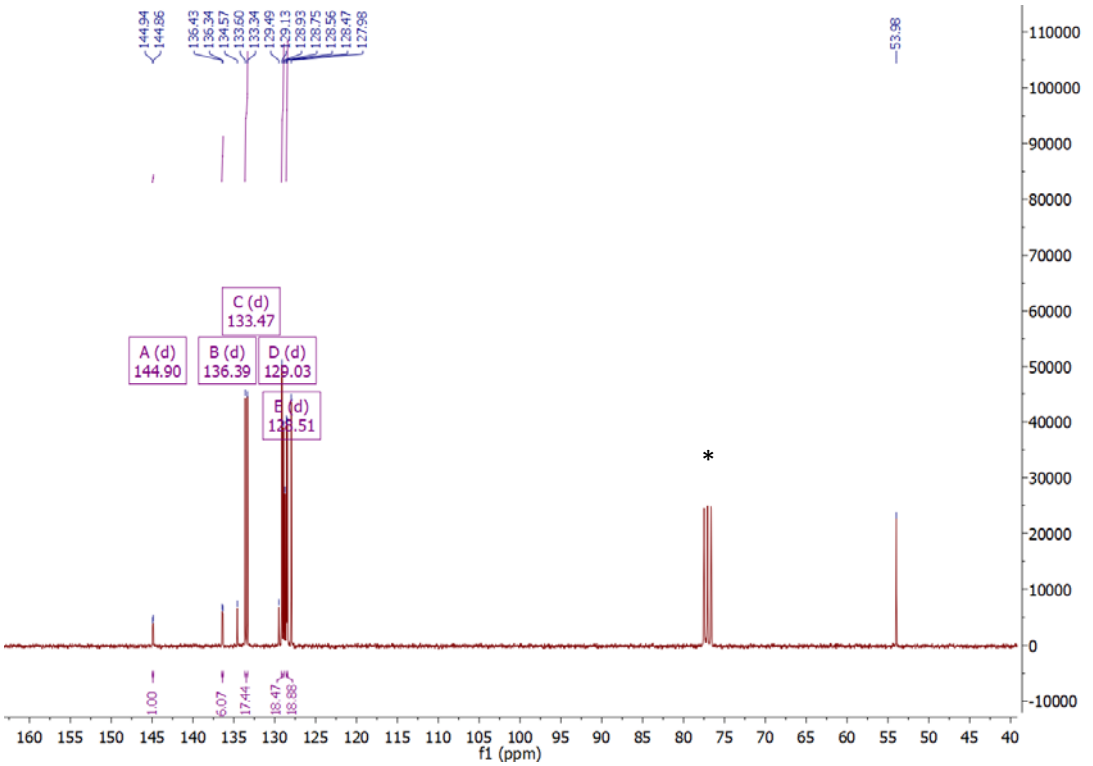

Figure S22. ^{13}C NMR (75 MHz, $CDCl_3$, 298 K) spectrum of **4** (* = solvent peak).

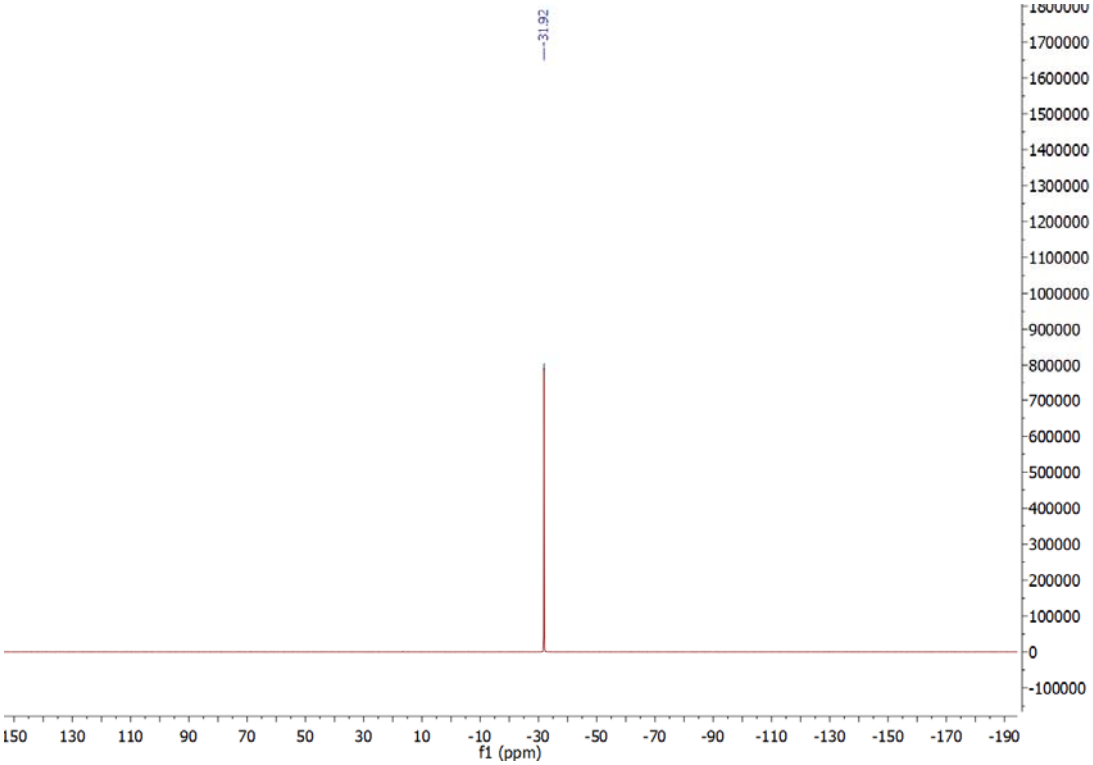

Figure S23. $^{31}P\{^1H\}$ NMR (121 MHz, $CDCl_3$, 298 K) spectrum of **4**.

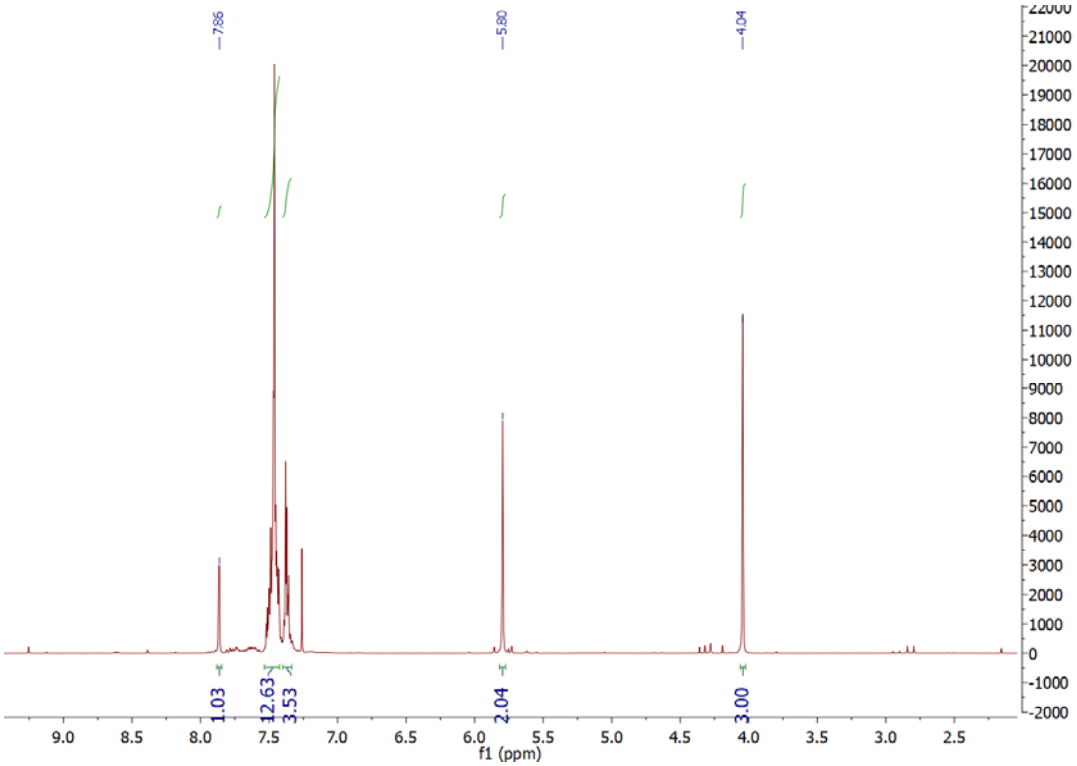

Figure S24. ^{1}H NMR (300 MHz, $CDCl_3$, 298 K) spectrum of **5**.

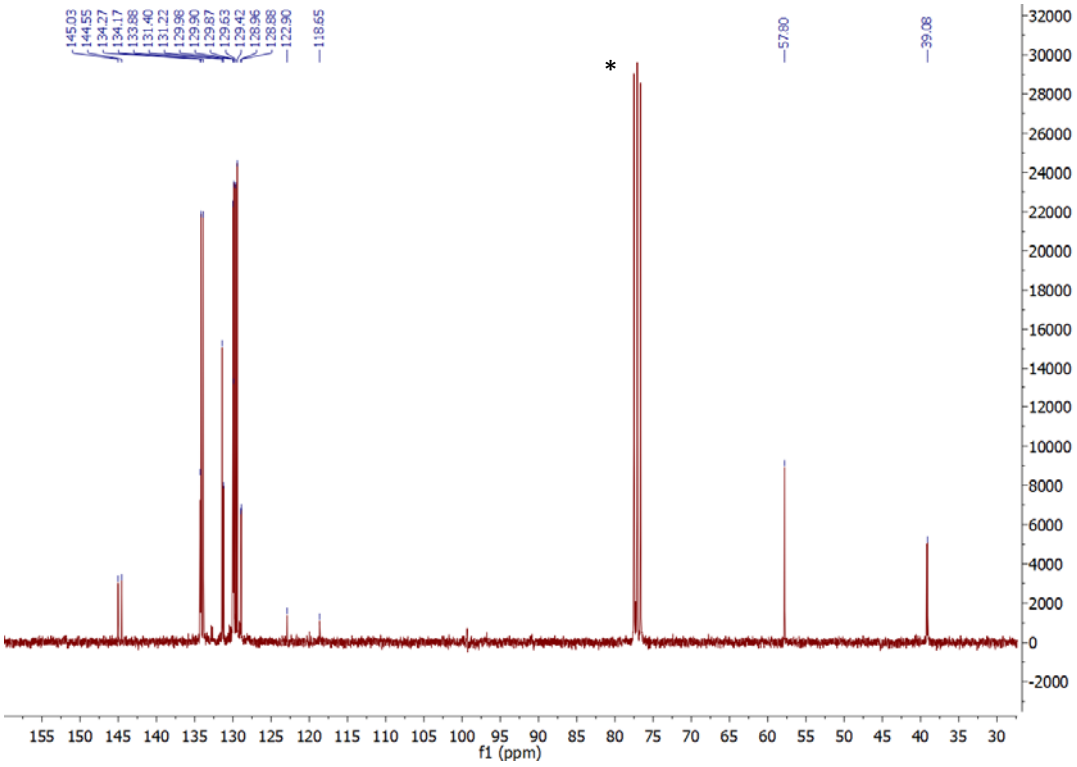

Figure S25. ^{13}C NMR (75 MHz, $CDCl_3$, 298 K) spectrum of **5** (* = solvent peak).

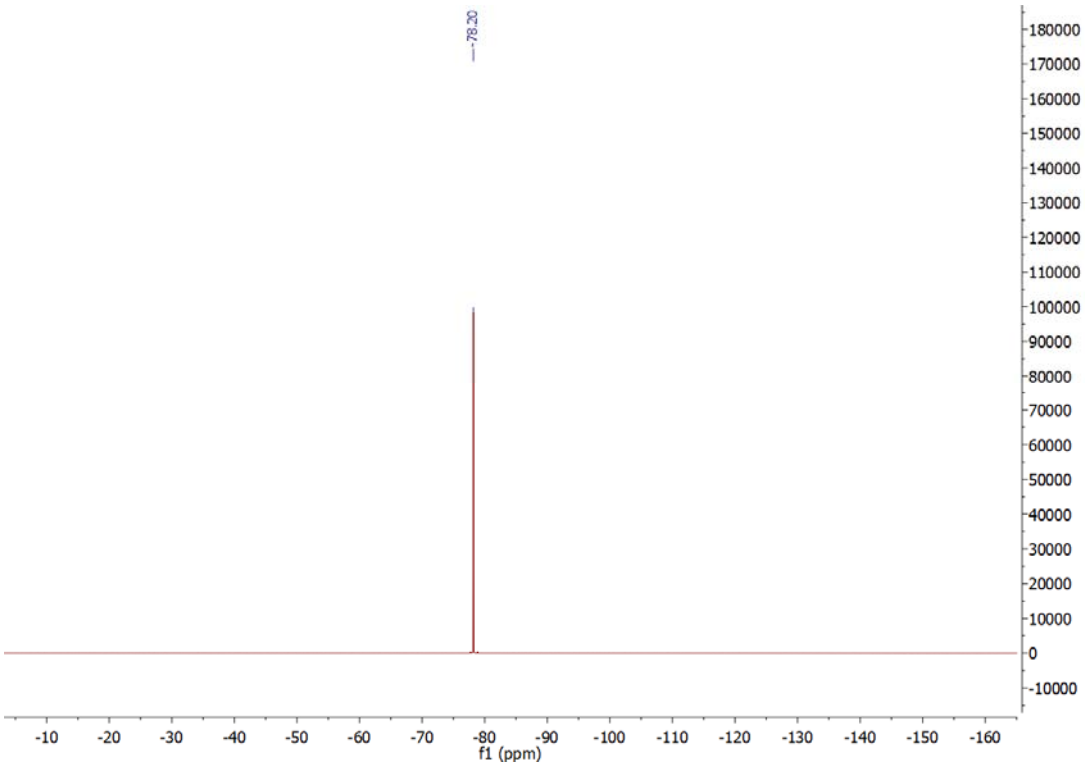

Figure S26. ^{19}F NMR (282 MHz, $CDCl_3$, 298 K) spectrum of **5**.

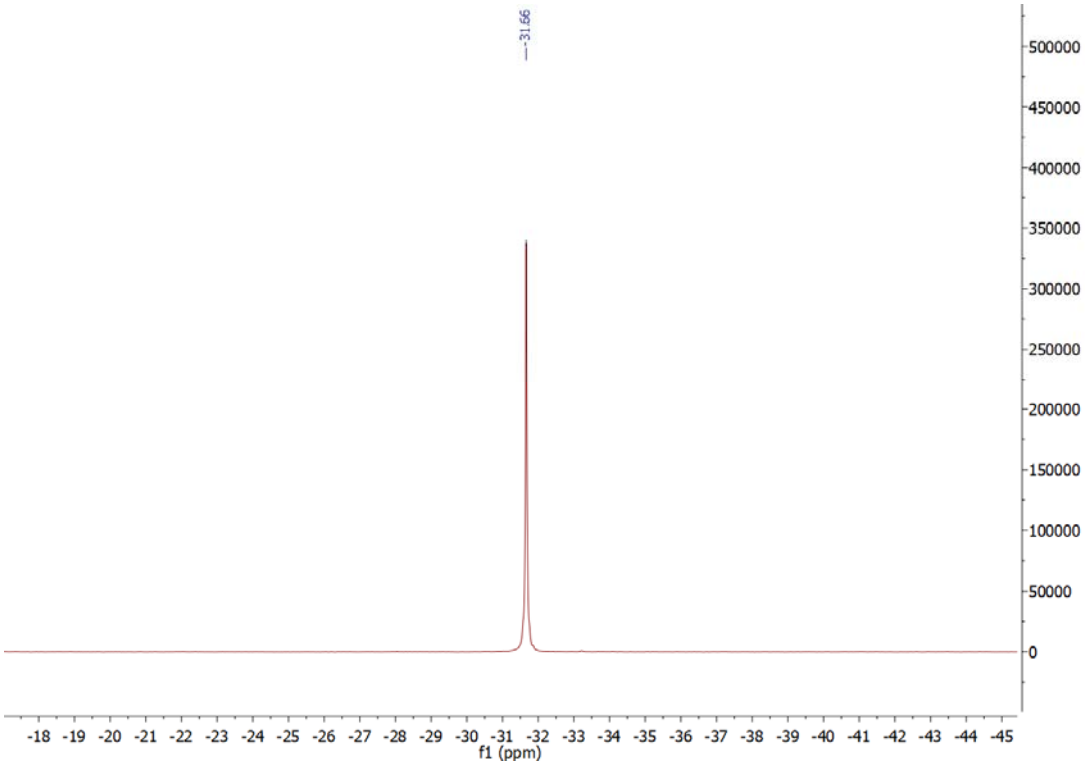

Figure S27. $^{31}P\{^1H\}$ NMR (121 MHz, $CDCl_3$, 298 K) spectrum of **5**.

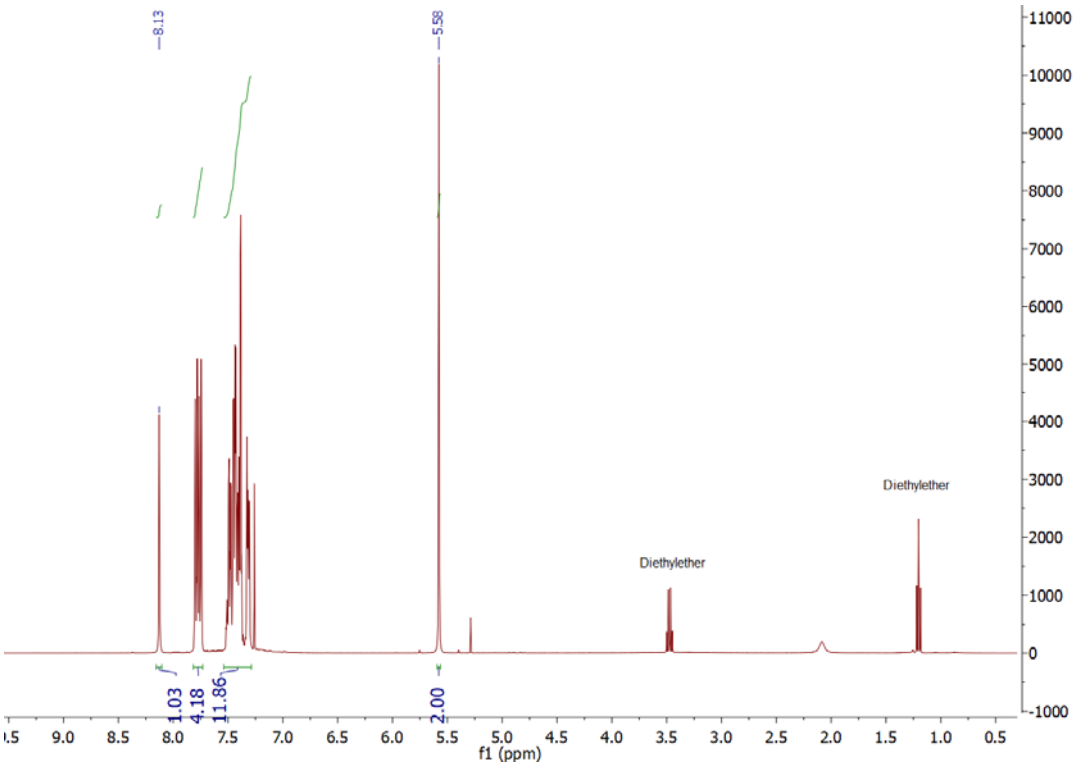

Figure S28. ^{1}H NMR (300 MHz, $CDCl_3$, 298 K) spectrum of **6**.

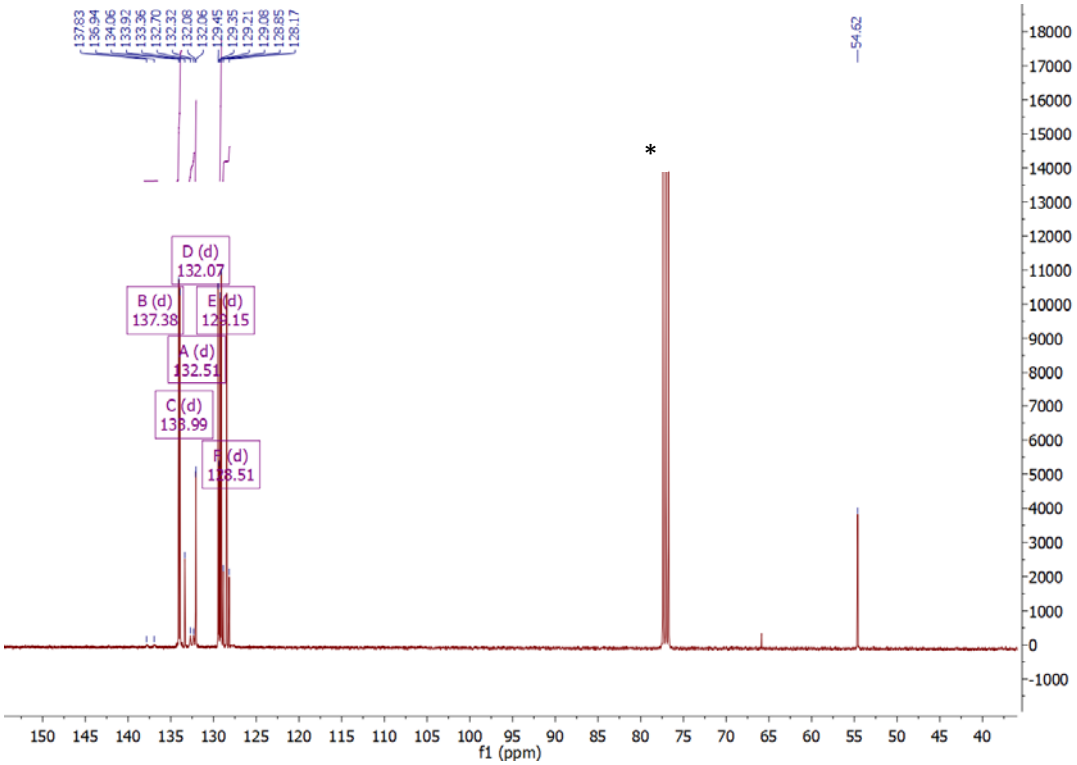

Figure S29. ^{13}C NMR (75 MHz, $CDCl_3$, 298 K) spectrum of **6** (* = solvent peaks).

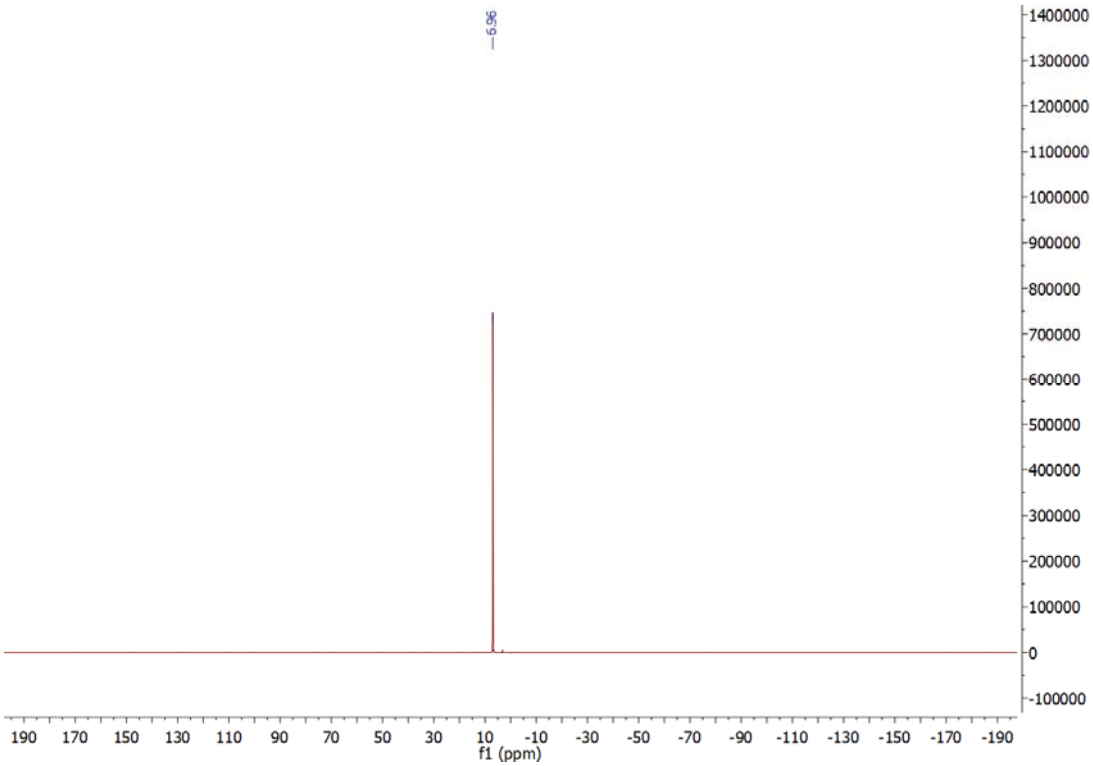

Figure S30. $^{31}P\{^{1}H\}$ NMR (121 MHz, $CDCl_3$, 298 K) spectrum of **6**.

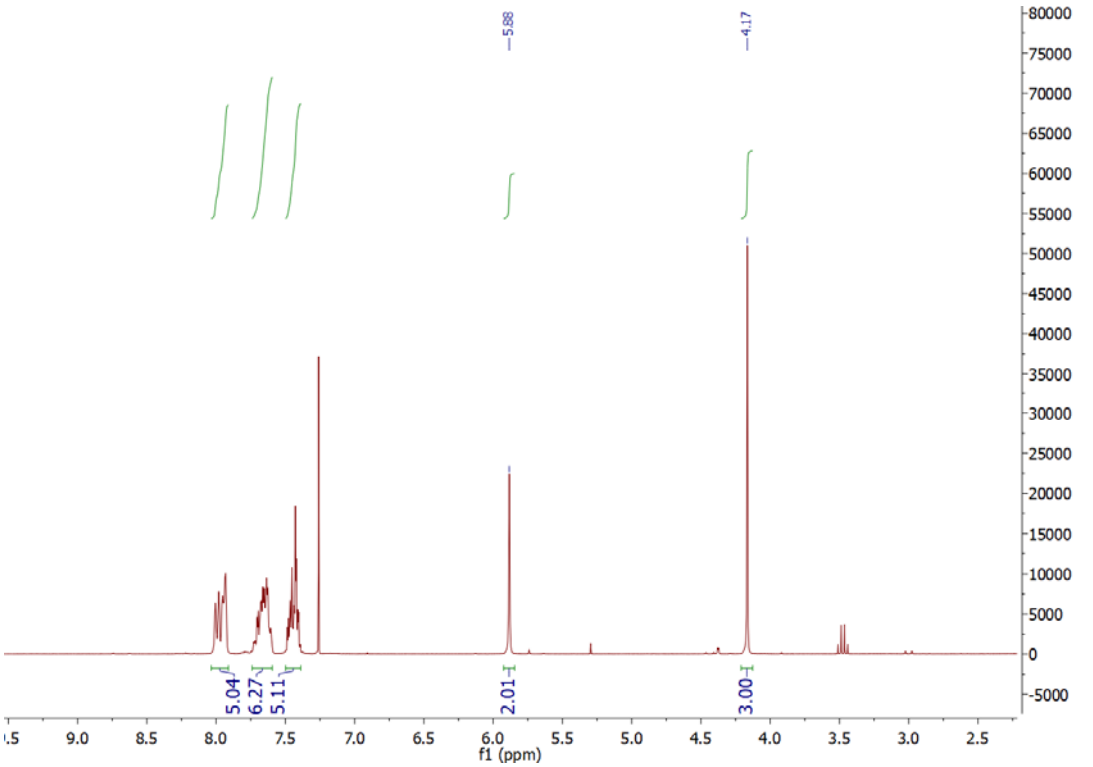

Figure S31. ^{1}H NMR (300 MHz, $CDCl_3$, 298 K) spectrum of **7**

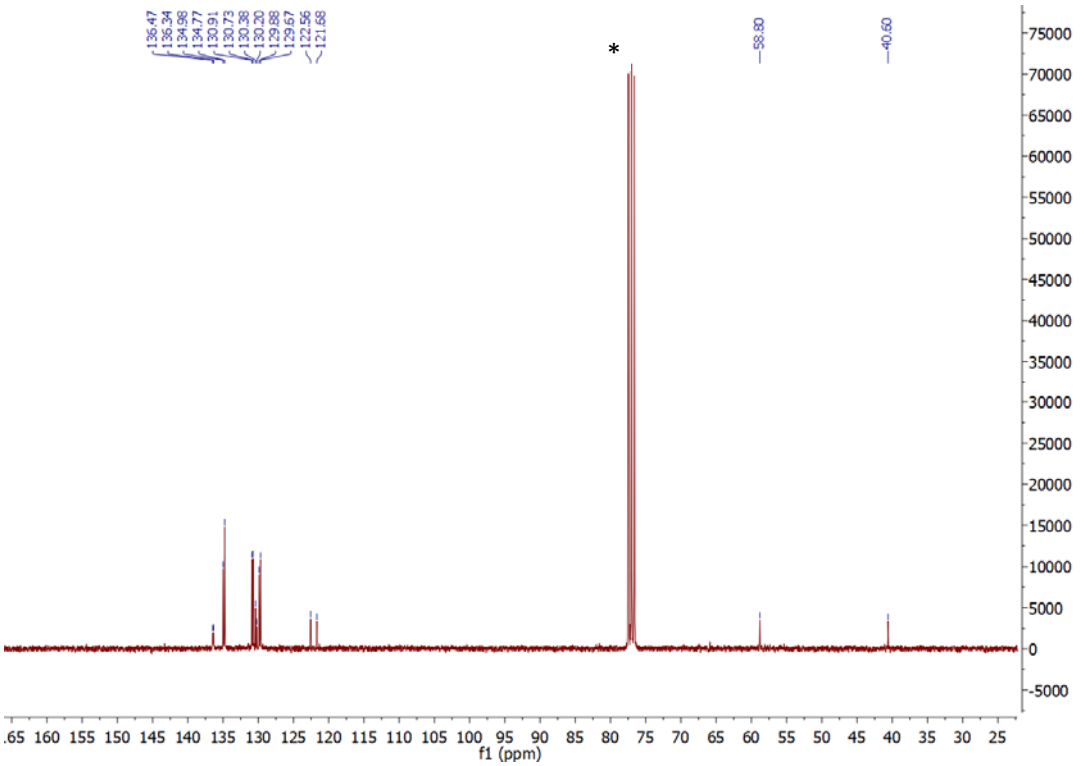

Figure S32. ^{13}C NMR (75 MHz, $CDCl_3$, 298 K) spectrum of **7** (* = solvent peak).

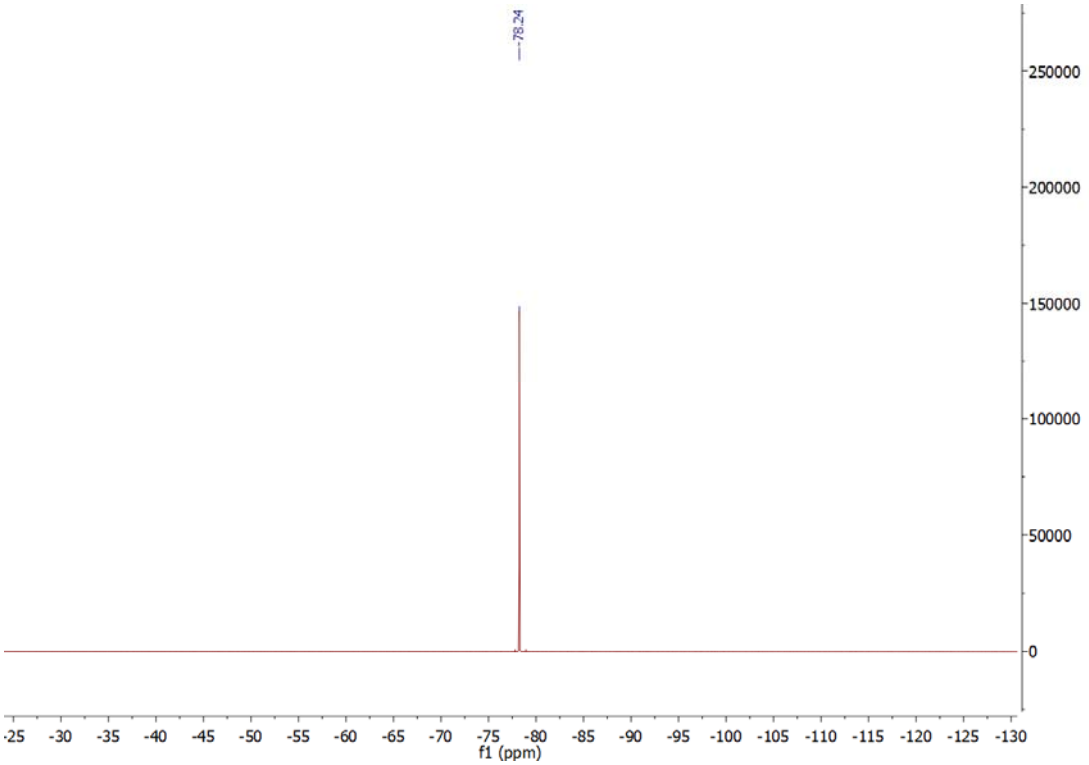

Figure S33. ^{19}F NMR (282 MHz, $CDCl_3$, 298 K) spectrum of **7**.

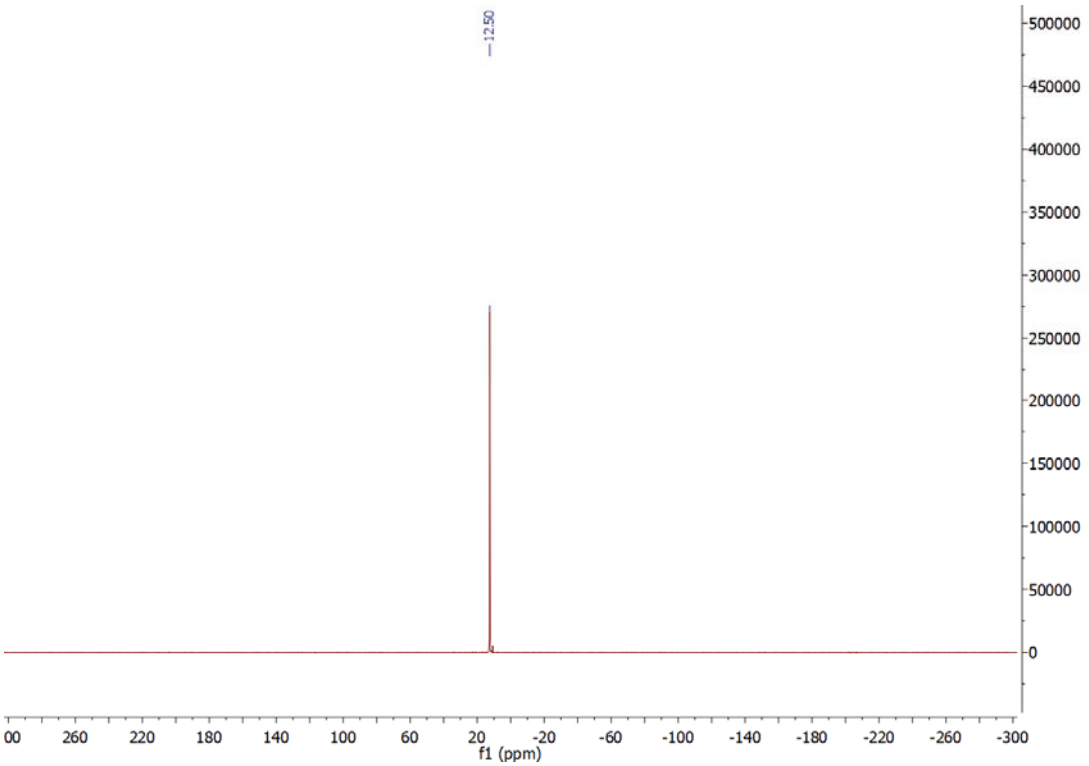

Figure S34. $^{31}P\{^{1}H\}$ NMR (121 MHz, $CDCl_3$, 298 K) spectrum of **7**.

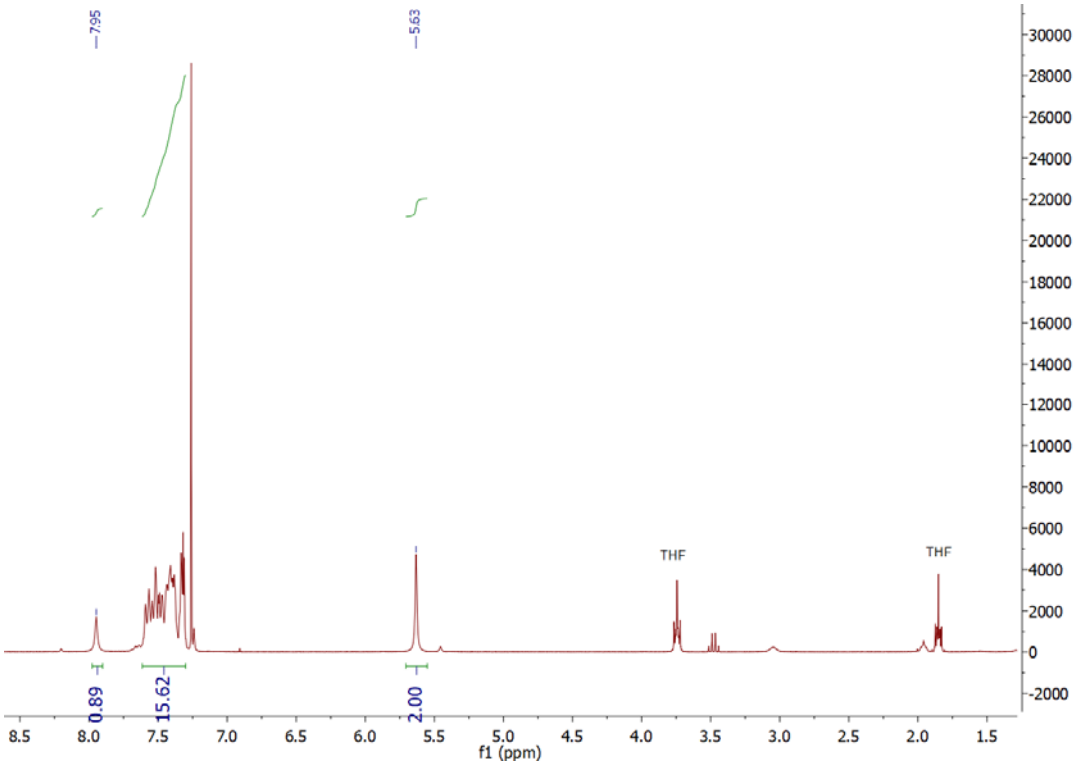

Figure S35. ^{1}H NMR (300 MHz, $CDCl_3$, 298 K) spectrum of **8** (* = solvent peaks).

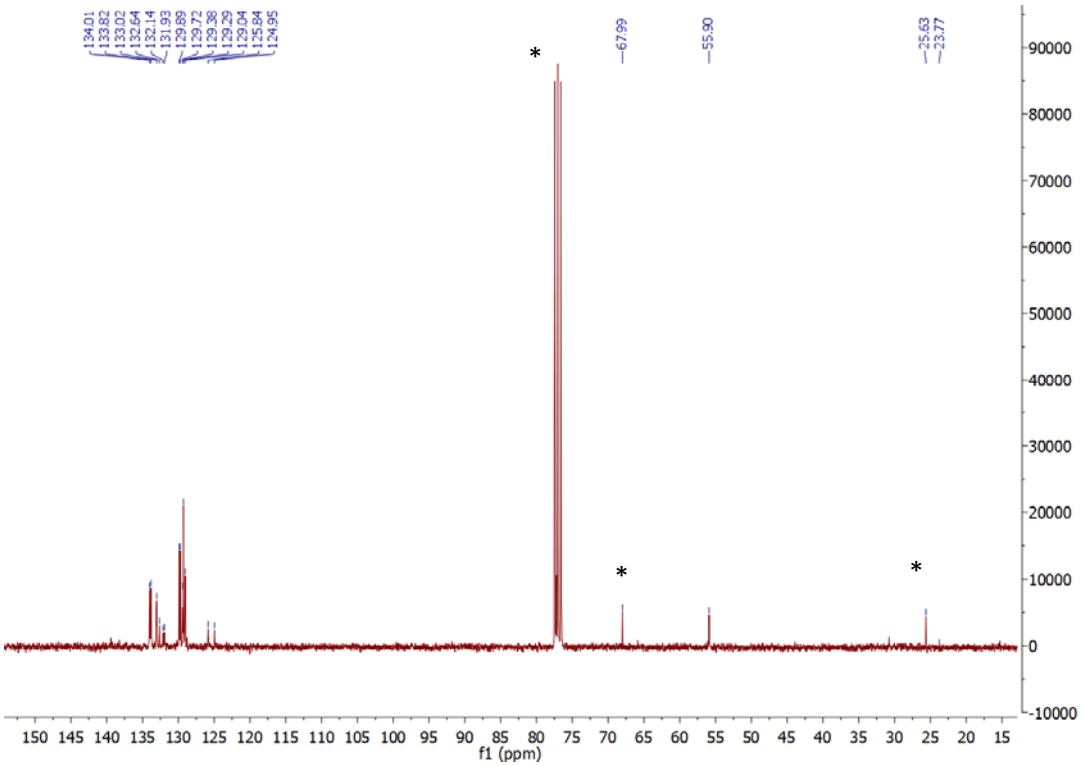

Figure S36. ^{13}C NMR (75 MHz, $CDCl_3$, 298 K) spectrum of **8** (* = solvent peaks).

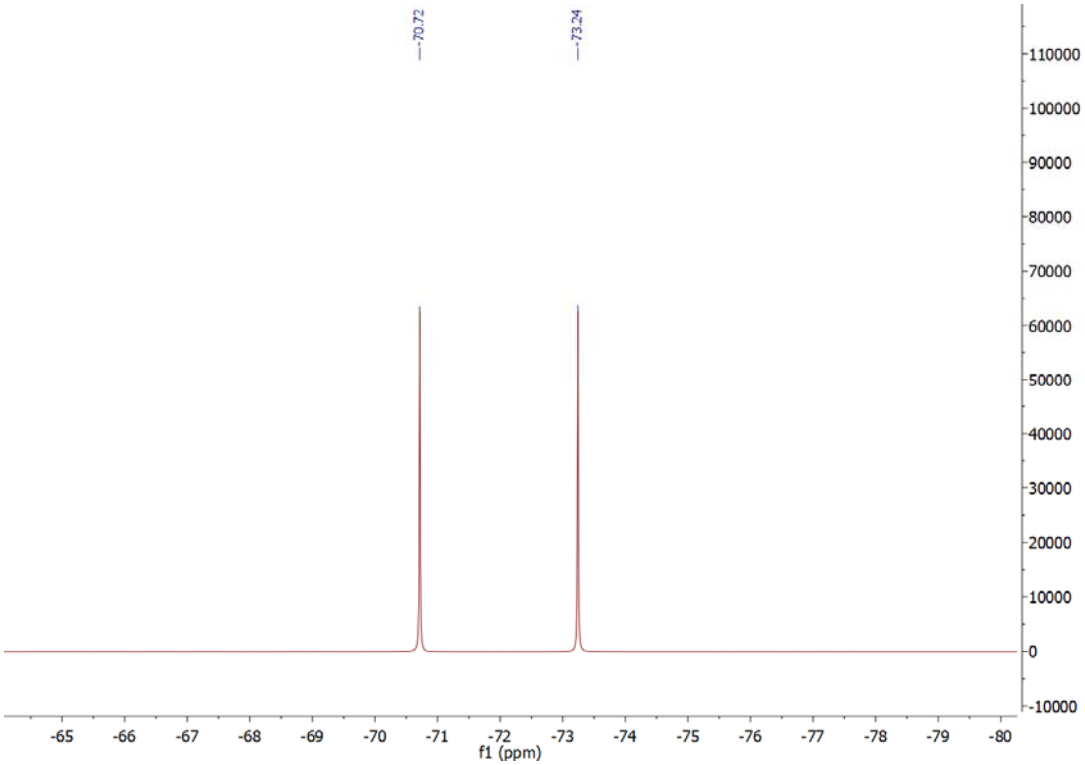

Figure S37. ^{19}F NMR (282 MHz, $CDCl_3$, 298 K) spectrum of **8**.

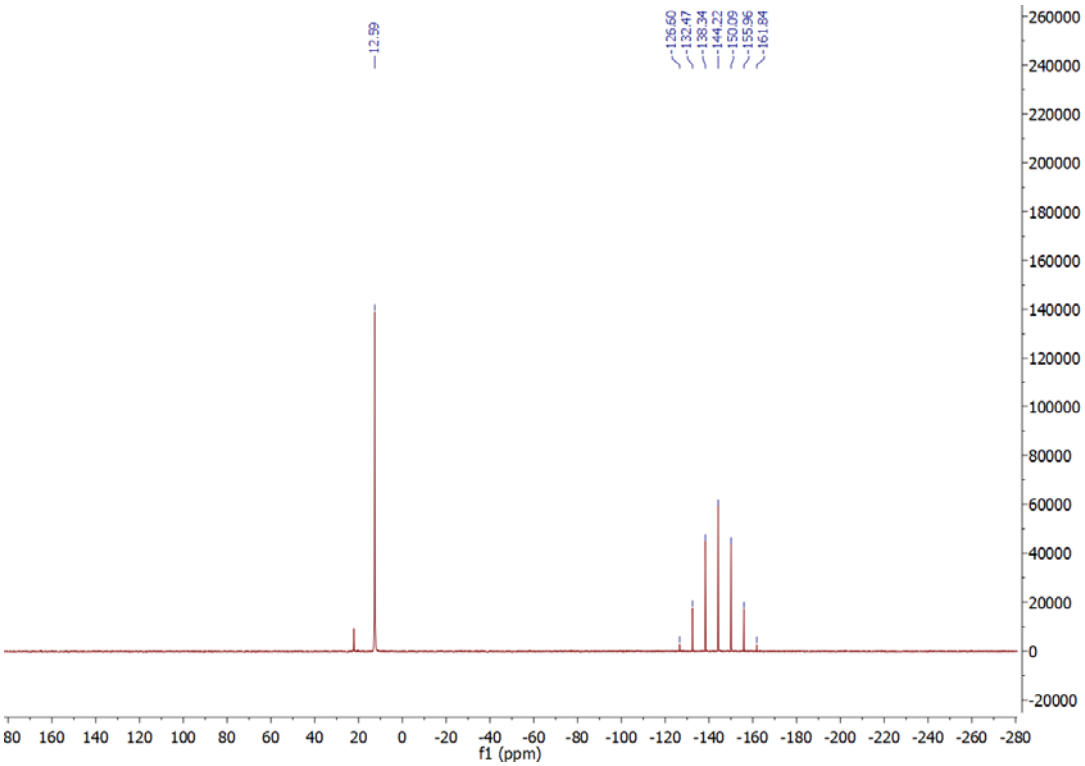

Figure S38. $^{31}P\{^{1}H\}$ NMR (121 MHz, $CDCl_3$, 298 K) spectrum of **8**.

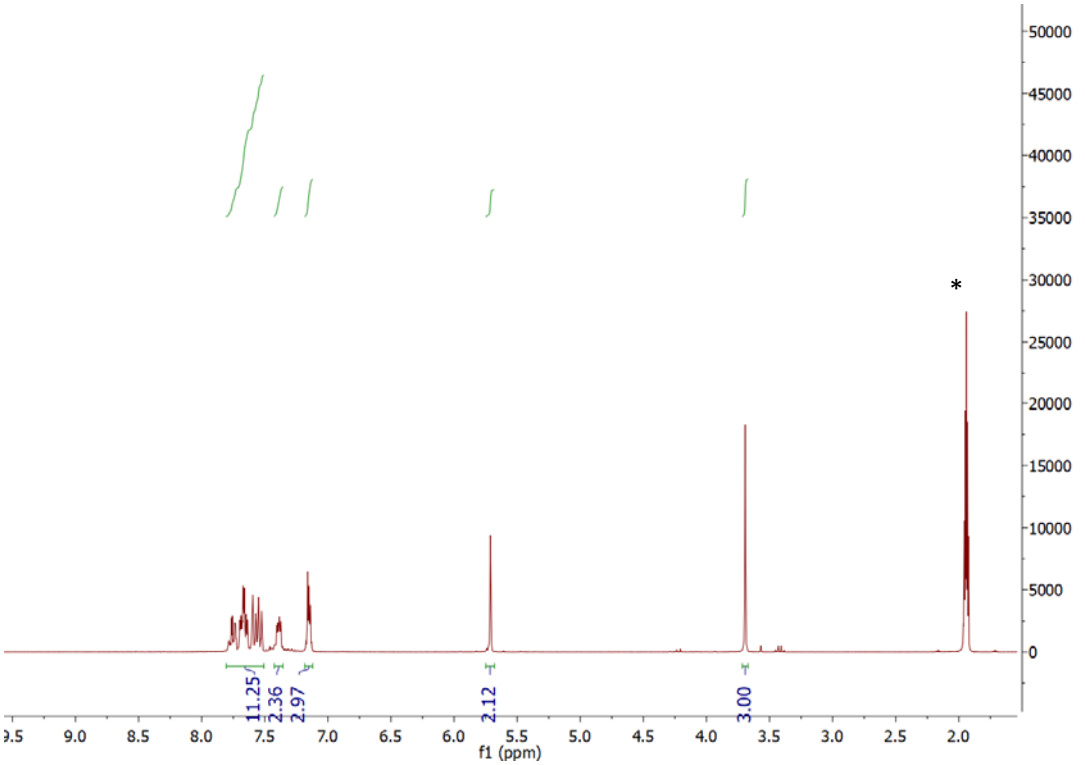

Figure S39. ^{1}H NMR (300 MHz, CD_3CN, 298 K) spectrum of **9** (* = solvent peak).

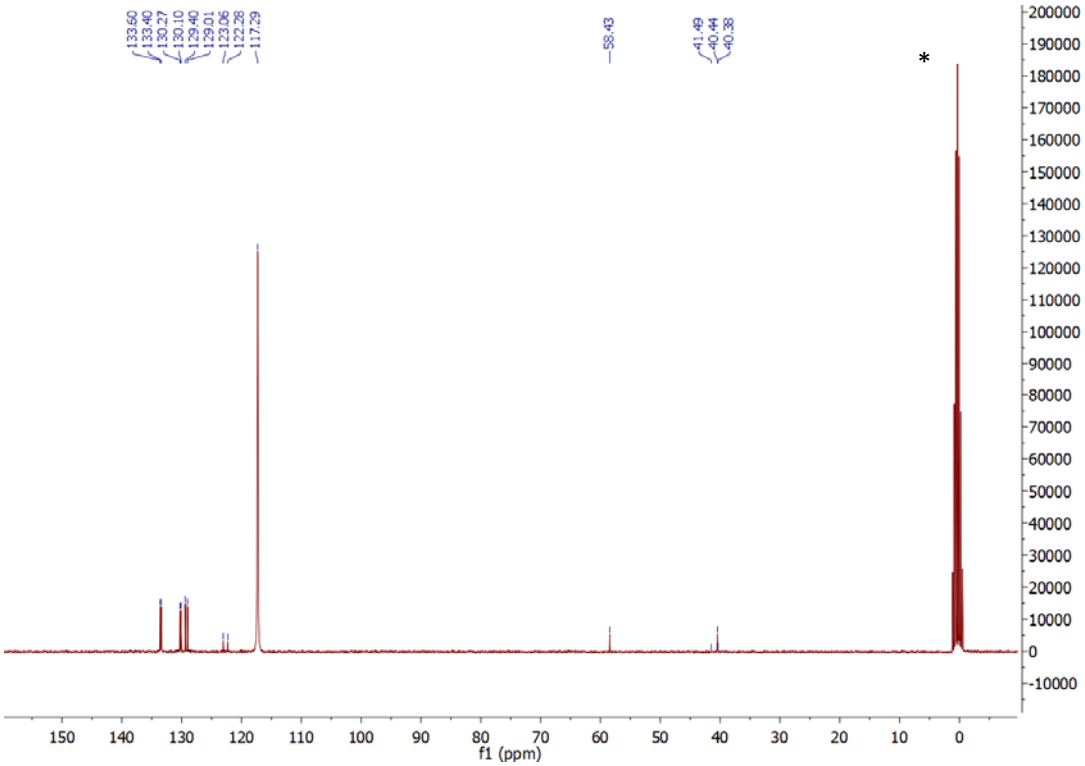

Figure S40. ^{13}C NMR (75 MHz, CD_3CN, 298 K) spectrum of **9** (* = solvent peak).

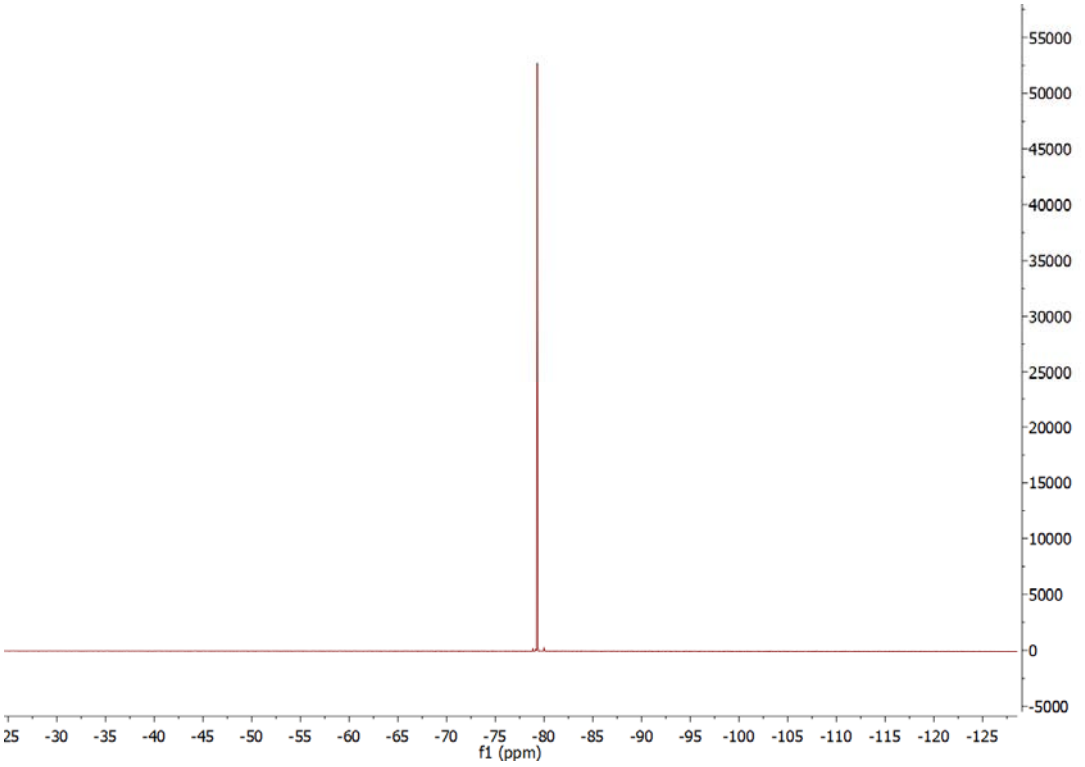

Figure S41. ^{19}F NMR (282 MHz, CD_3CN, 298 K) spectrum of **9**.

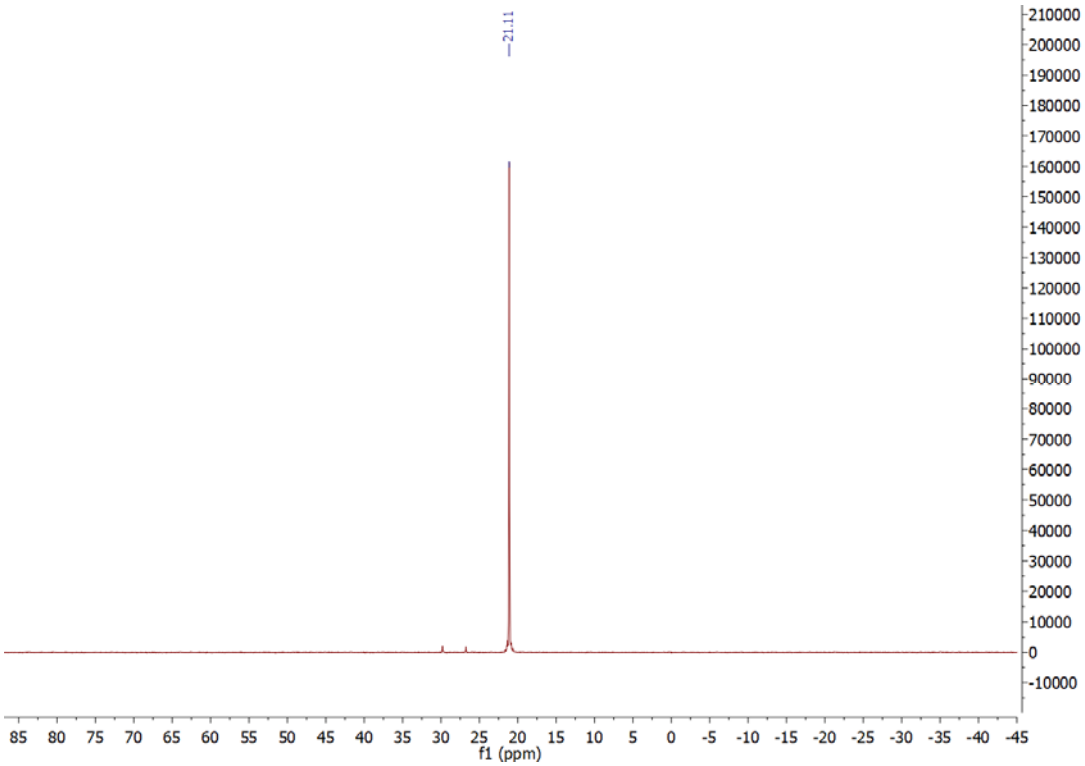

Figure S42. $^{31}P\{^{1}H\}$ NMR (121 MHz, CD_3CN, 298 K) spectrum of **9**.

5. IR Spectra

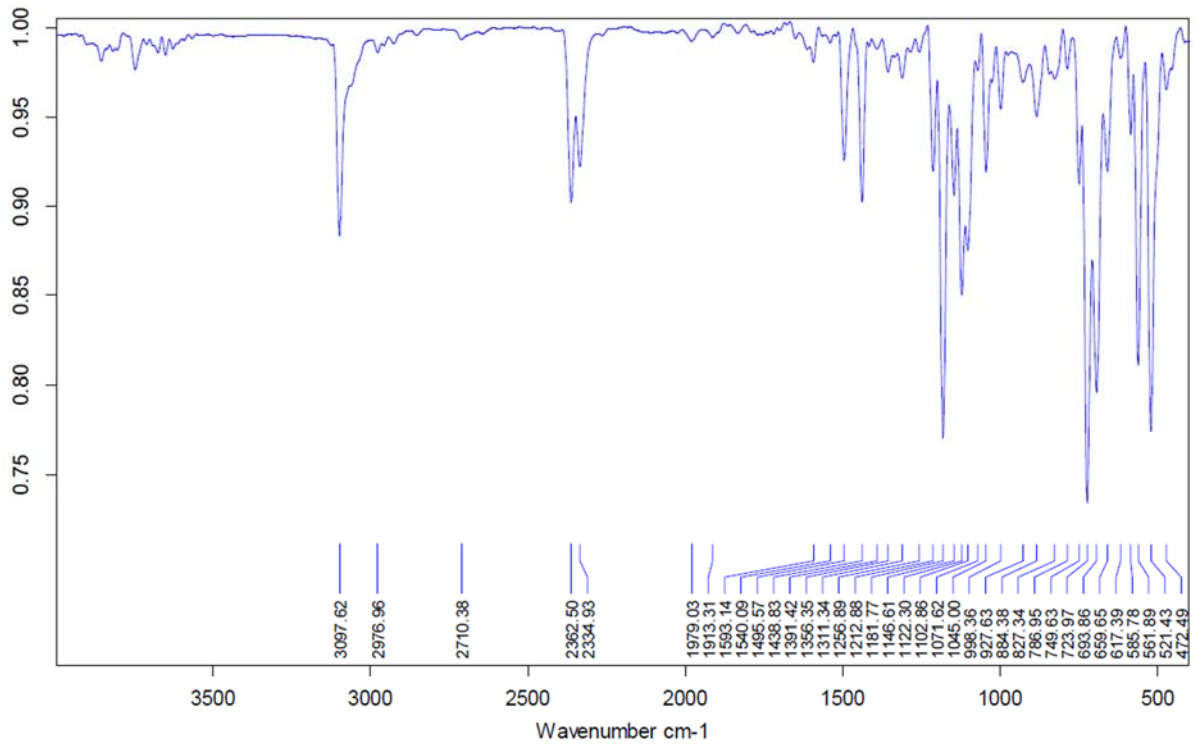

Figure S43. IR (ATR) spectrum of **2**.

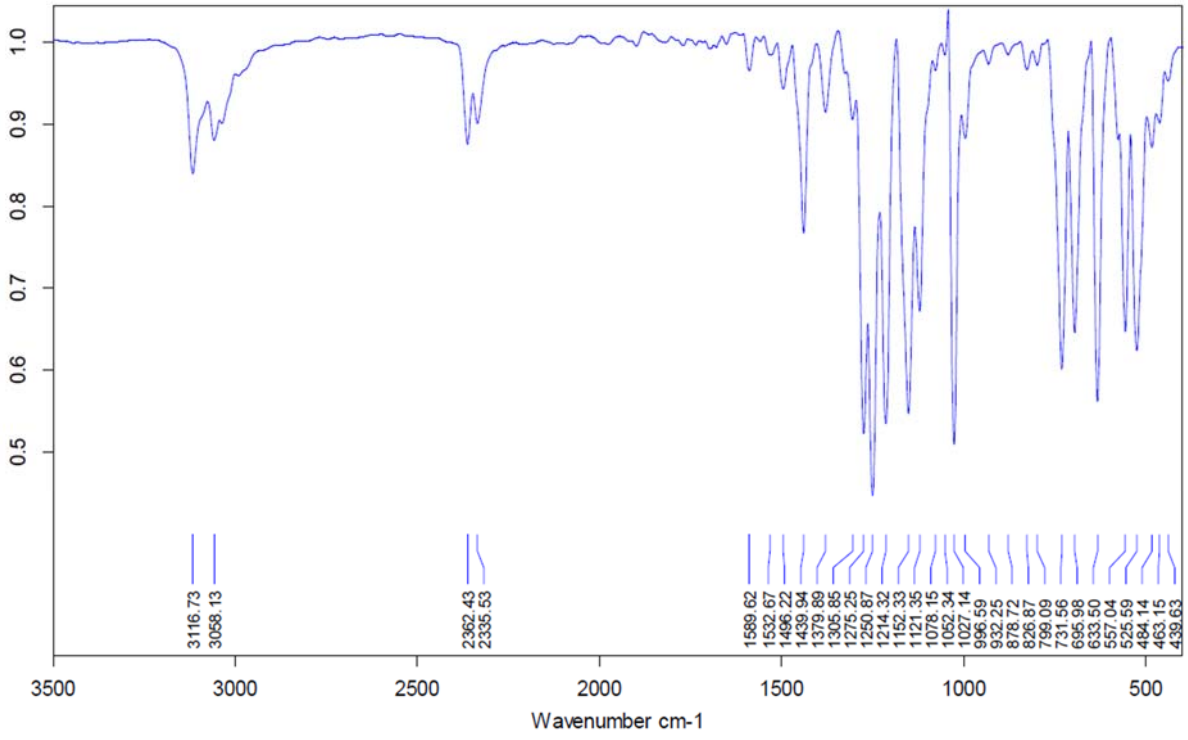

Figure S44. IR (ATR) spectrum of **3**.

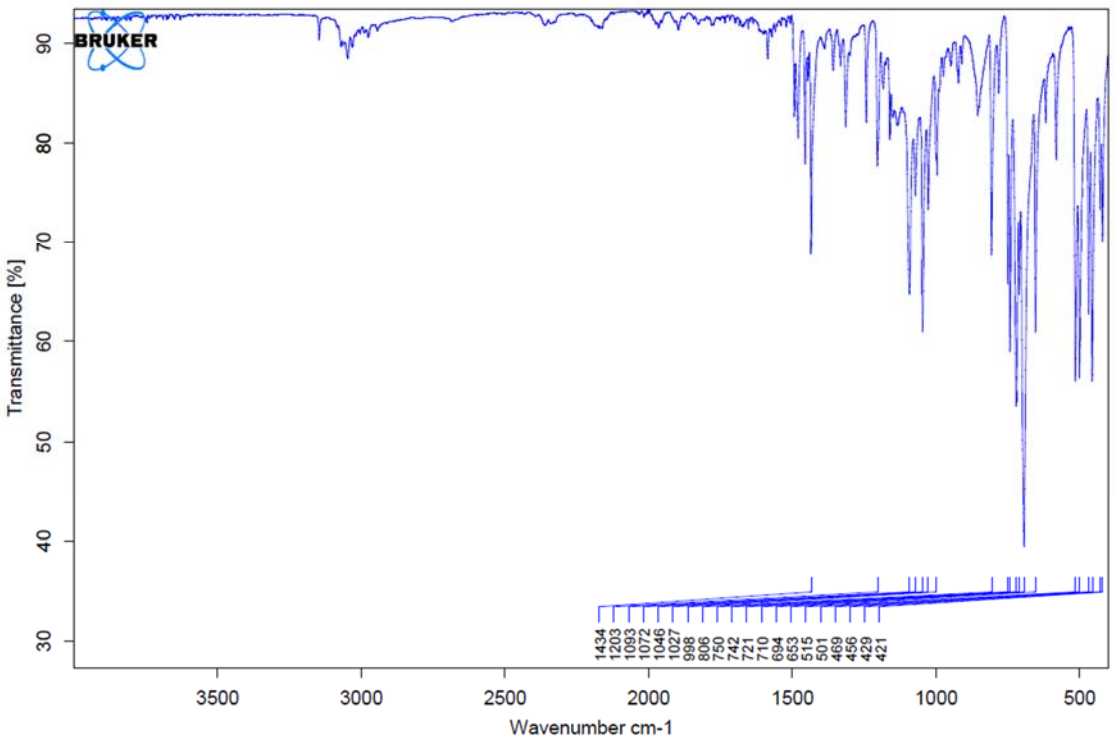

Figure S45. IR (ATR) spectrum of **4**.

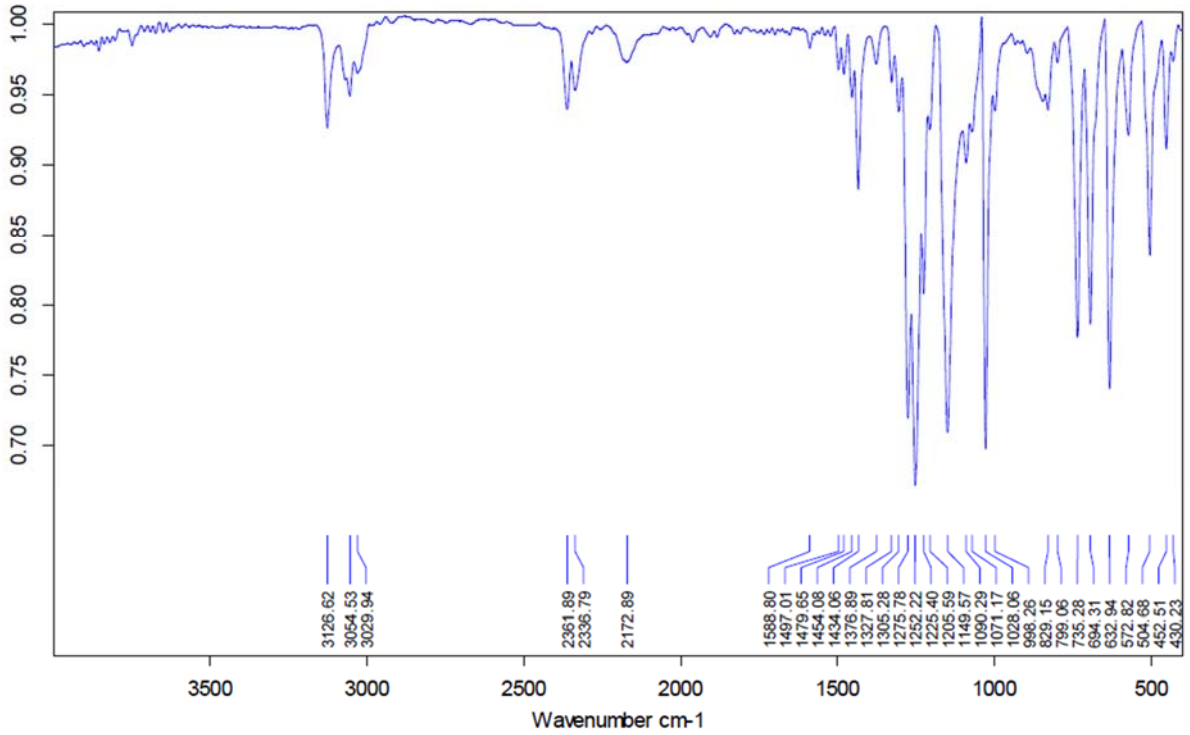

Figure S46. IR (ATR) spectrum of **5.**

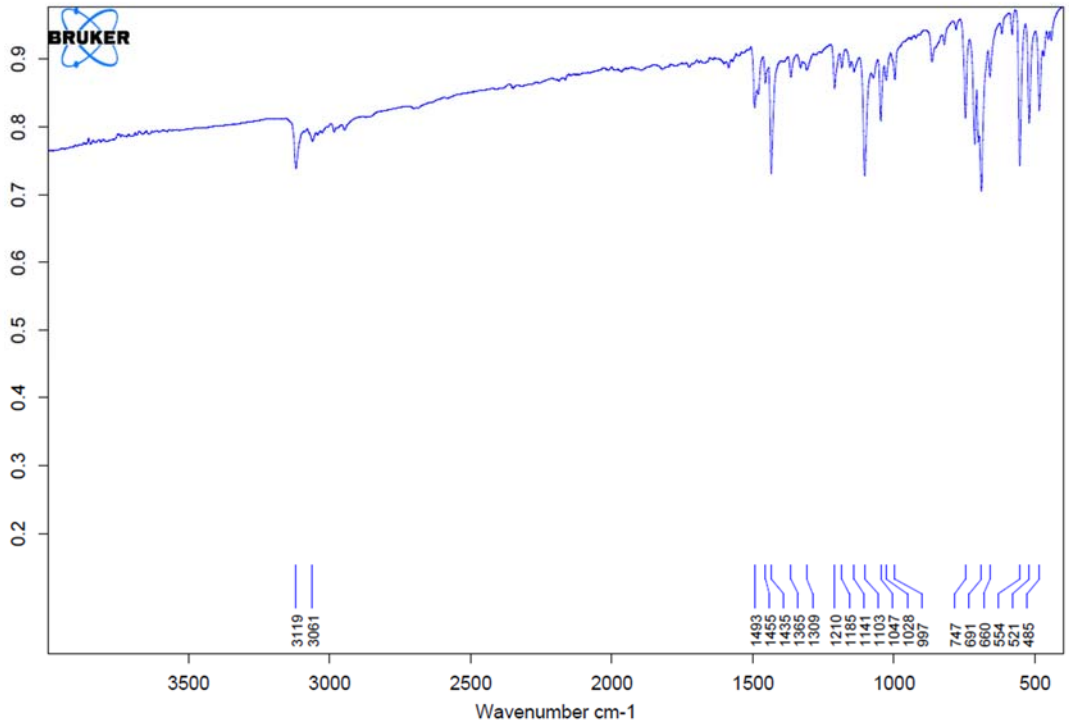

Figure S47. IR (ATR) spectrum of **6**.

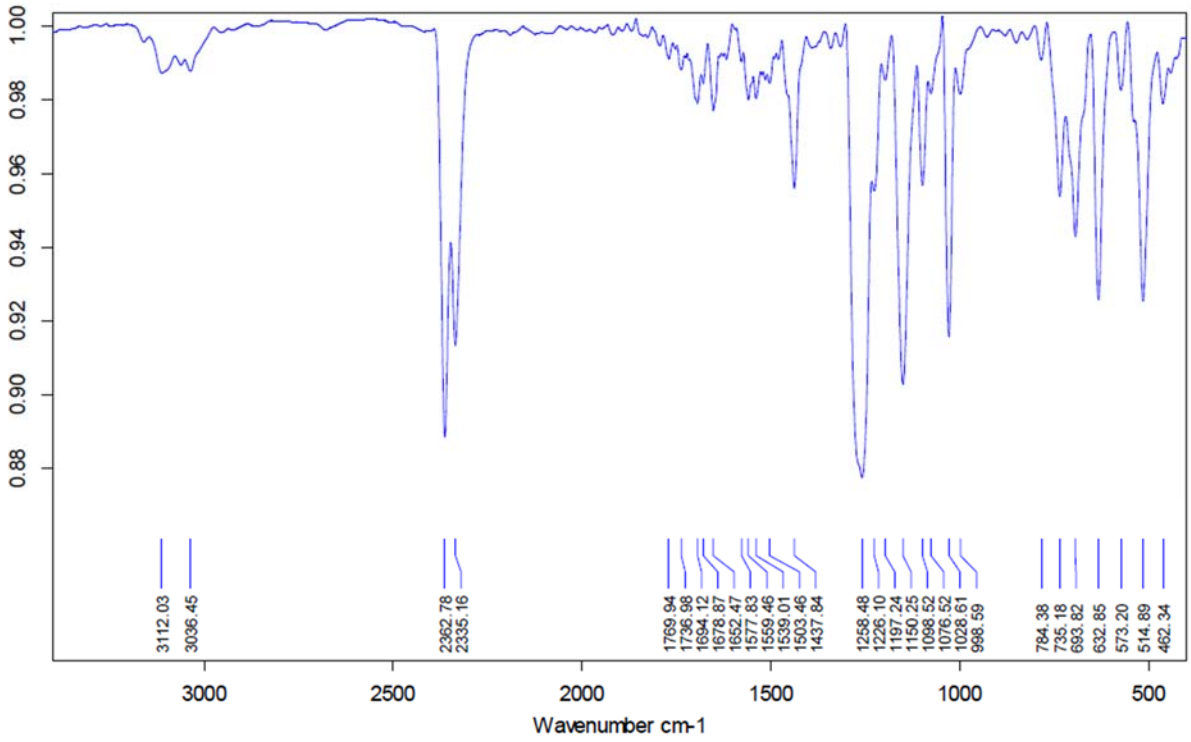

Figure S48. IR (ATR) spectrum of **7**.

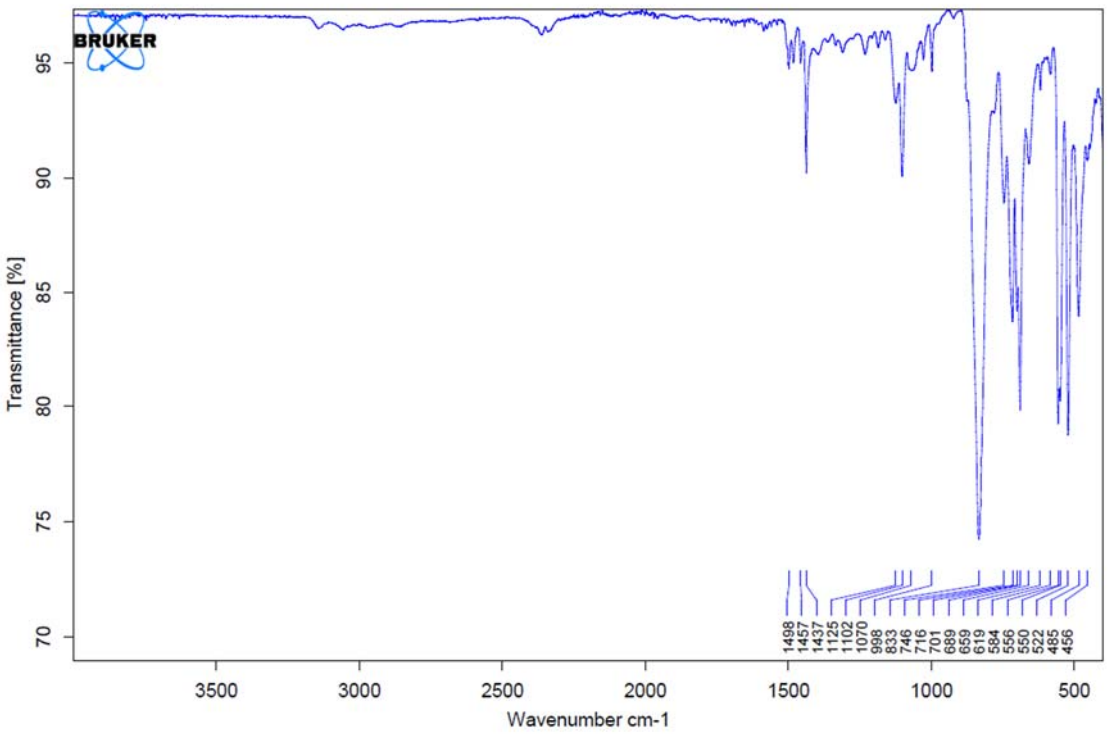

Figure S49. IR (ATR) spectrum of **8**

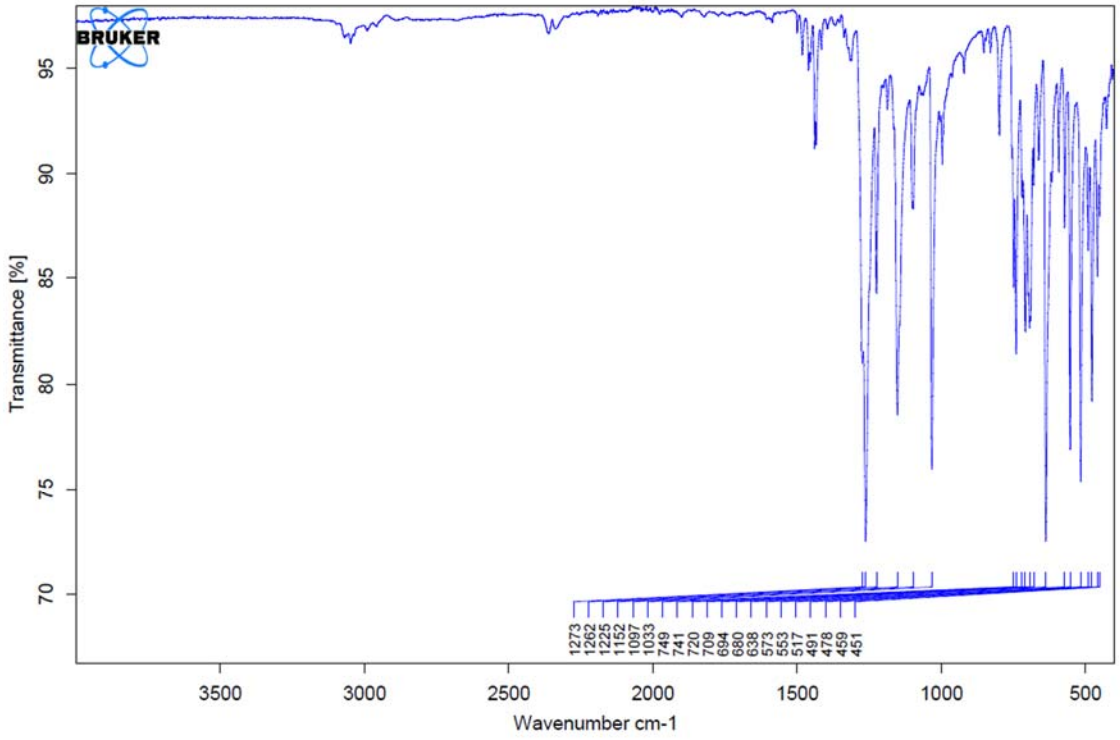

Figure S50. IR (ATR) spectrum of **9**.

6. Mass Spectra

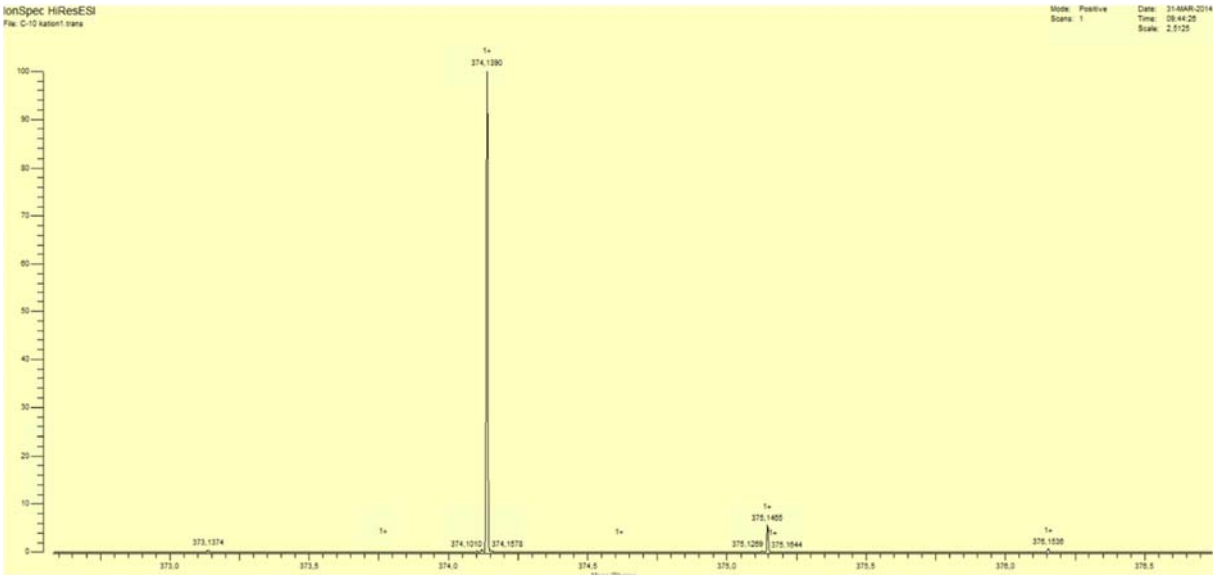

Figure S51. ESI mass spectrum of **3**. *m/z* = calcd. for $[M]^+$ 374.1422; found: 374.1390.

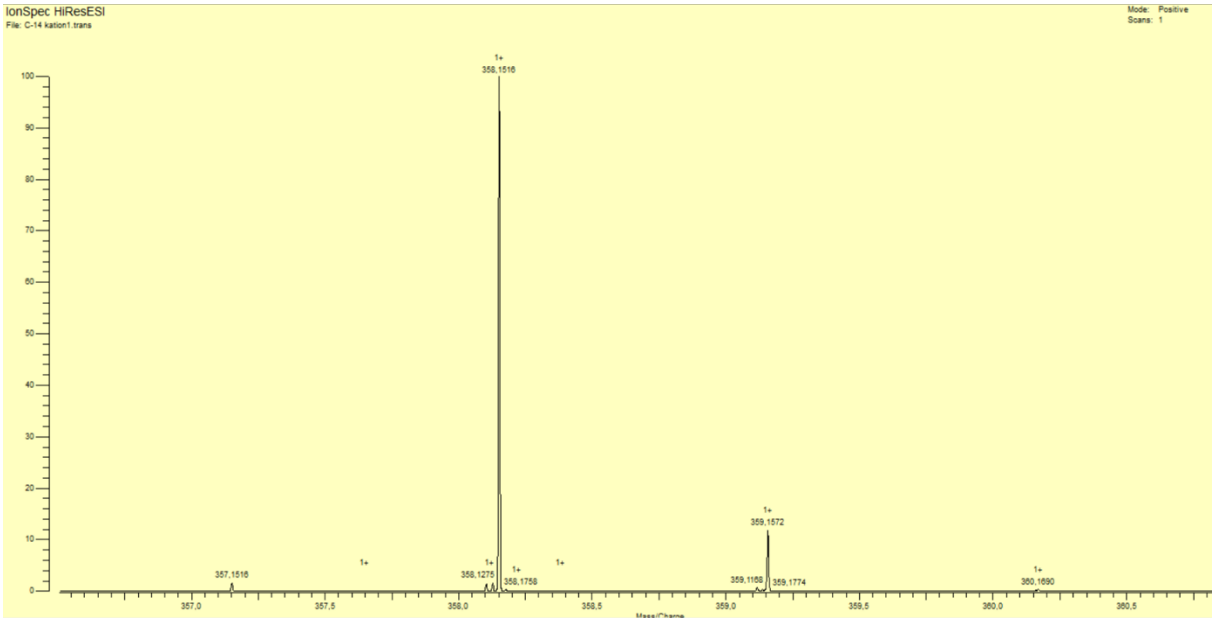

Figure S52. ESI mass spectrum of **5**. *m/z* = calcd. for $[M]^+$ 358.1473; found: 358.1516.

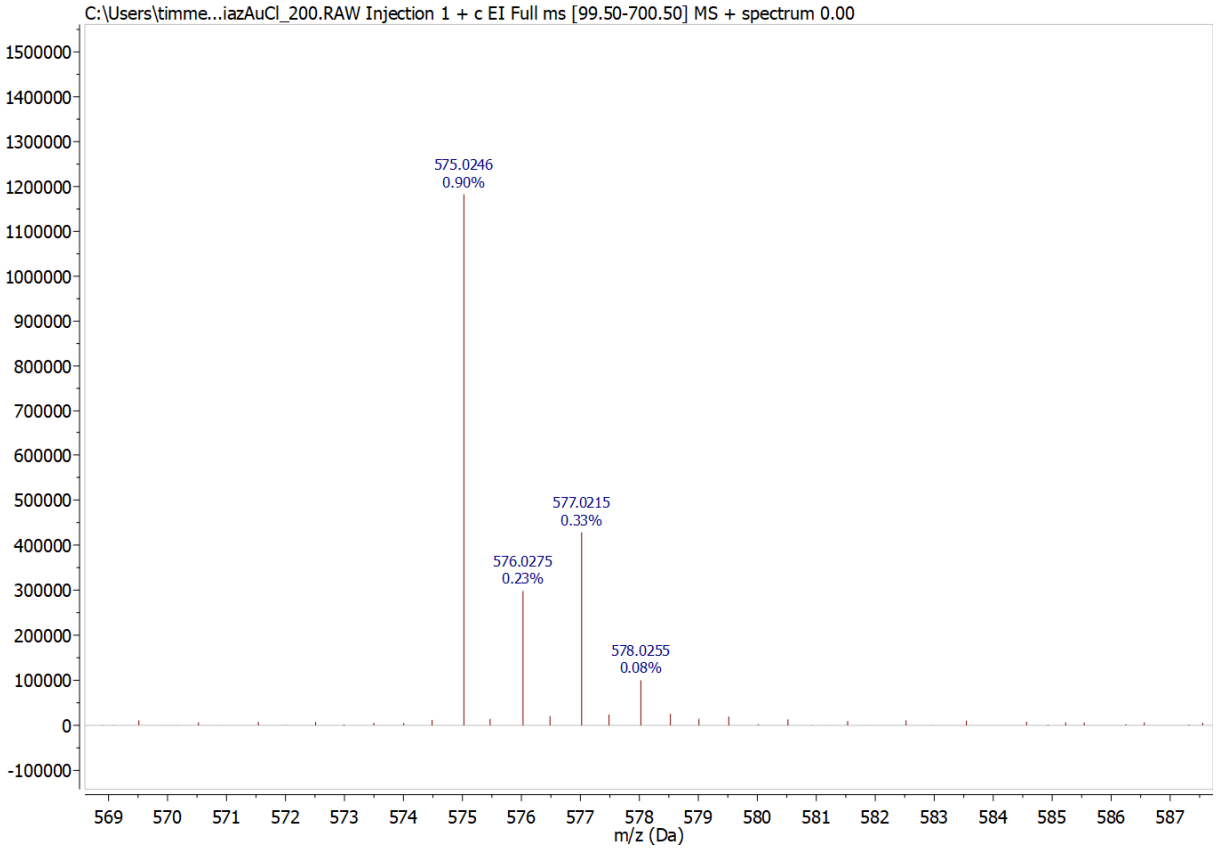

Figure S53. EI mass spectrum of **6**. *m/z* = calcd. for $[M]^+$ 575.0592; found: 575.0246.

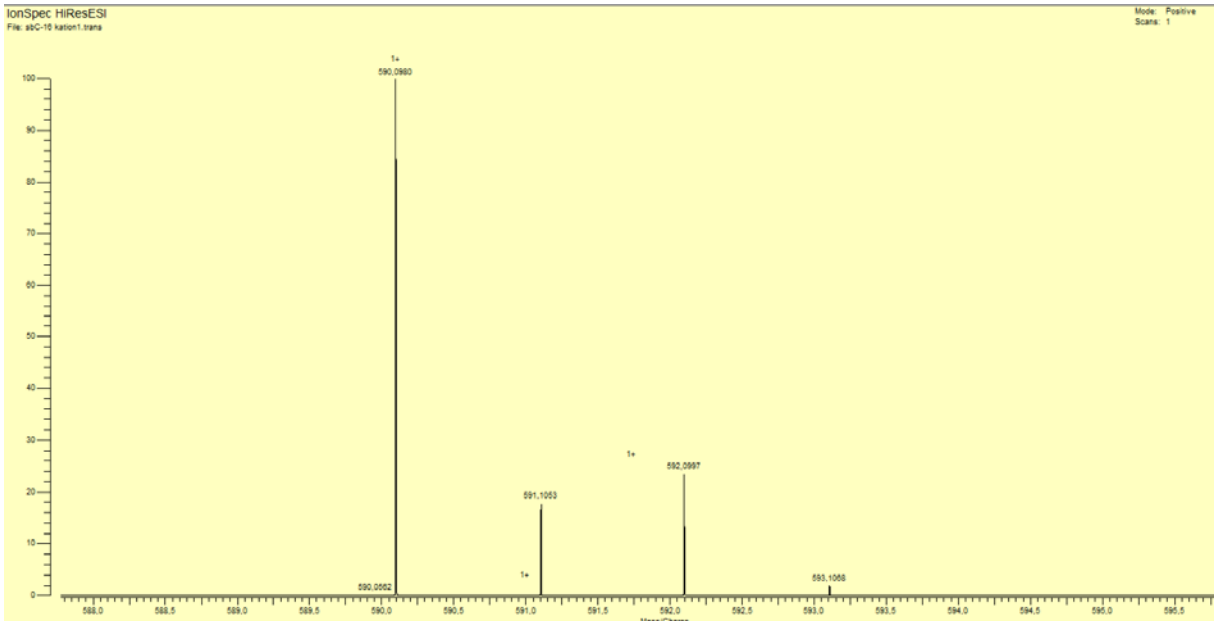

Figure S54. ESI mass spectrum of **7**. *m/z* = calcd. for $[M]^+$ 590,0827; found: 590.0980.

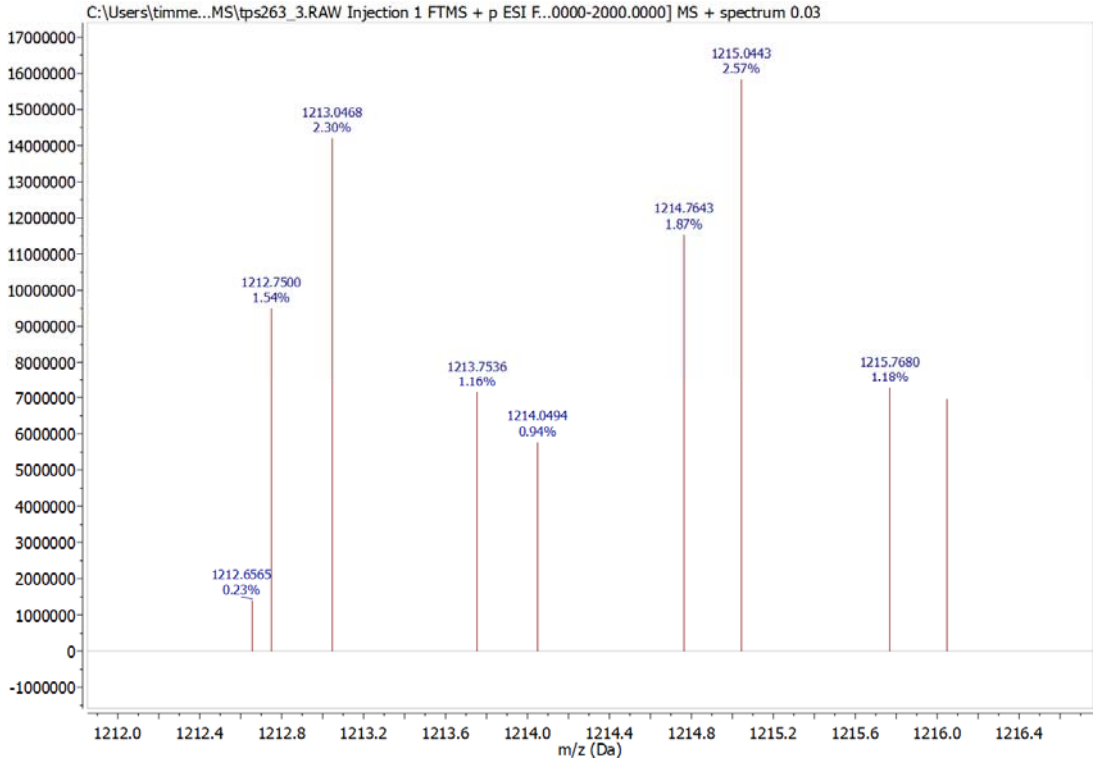

Figure S55. ESI mass spectrum of **8**. *m/z* = calcd. for $[M]^+$ 1213.0481; found: 1213.0468.

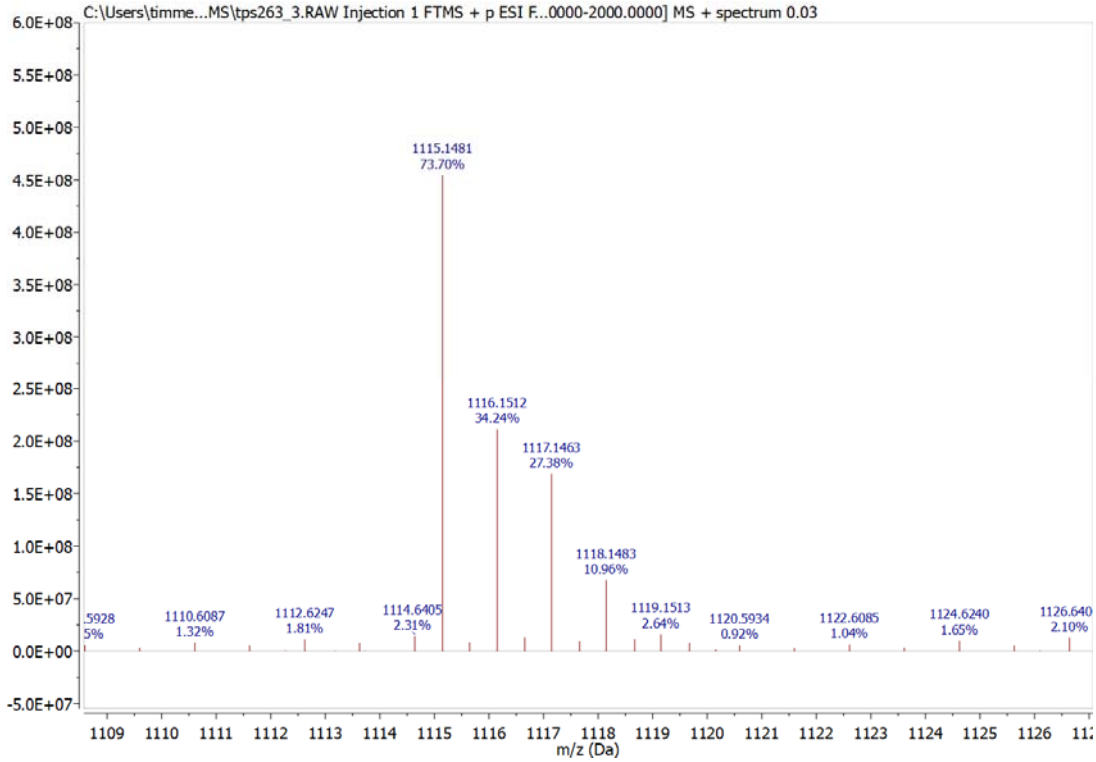

Figure S56. ESI mass spectrum of **8**. *m/z* = calcd. for $[(AuCl(L^{PN}))_2{-}Cl]^+$ 1115.1496; found: 1115.1481.

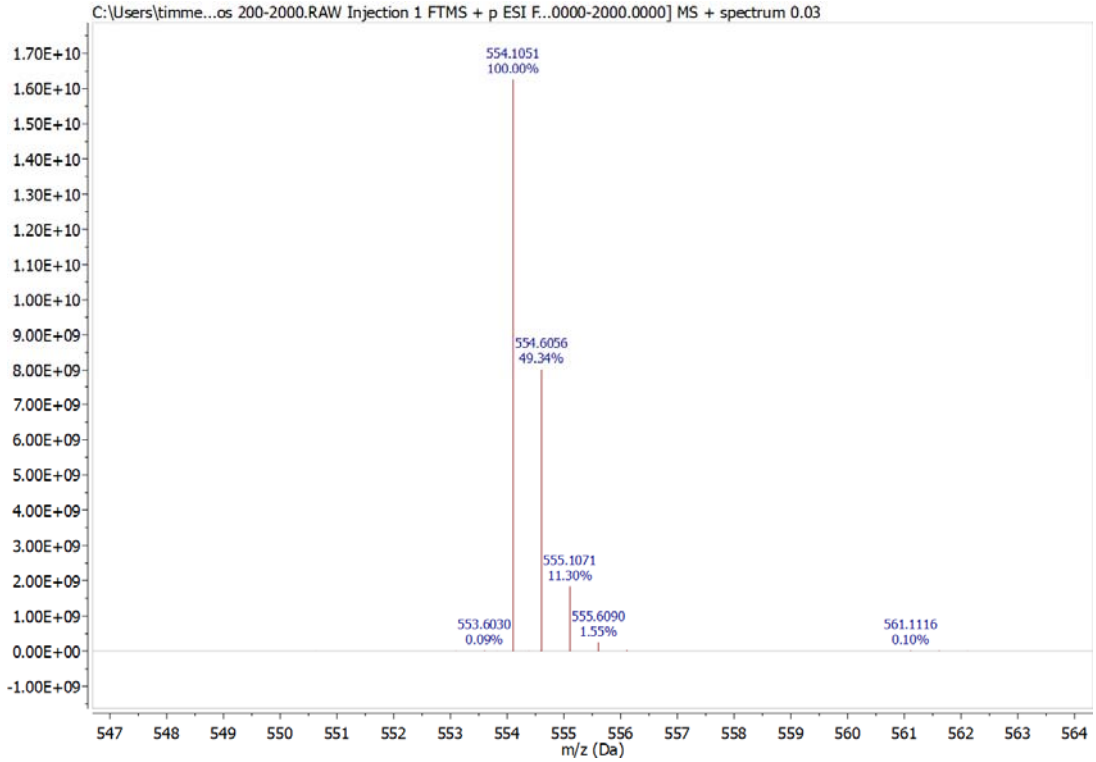

Figure S57. ESI mass spectrum of **9**. *m/z* = calcd. for $[M]^+$ 554.1060; found: 554.1051.

7. References

[1] J. C. De Mello, H. F. Wittmann, R. H. Friend, *Adv. Mater.* 1997, **9**, 230-232.

[2] L. Peng, F. Xu, K. Shinohara, T. Nishida, K. Wakamatsu, A. Orita, J. Otera, *Org. Chem. Front.* 2015, **2**, 248-252.

[3] R. Veillard, E. Bernoud, I. Abdellah, J.-F. Lohier, C. Alayrac, A.-C. Gaumont, *Org. Biomol. Chem.* 2014, **12**, 3635-3640.

[4] G. M. Sheldrick, *Acta Crystallogr. Sect. A* 2008, **64**, 112-122.

[5] G. M. Sheldrick, *Acta Crystallogr. Sect. C* 2015, **71**, 3-8.

[6] O. V. Dolomanov, L. J. Bourhis, R. J. Gildea, J. A. K. Howard, H. Puschmann, *J. Appl. Crystallogr.* 2009, **42**, 339-341.